

Probable chances of radioactive decays from superheavy nuclei $^{290-304}120$ within a modified generalized liquid drop model with a Q -value-dependent preformation factor

K. P. Santhosh[✉], Tinu Ann Jose, and N. K. Deepak

School of Pure and Applied Physics, Kannur University, Swami Anandatheertha Campus, Payyanur 670327, Kerala, India



(Received 19 January 2022; revised 24 March 2022; accepted 2 May 2022; published 16 May 2022)

All possible chances of heavy-cluster emissions are predicted for even-even isotopes of $^{290-304}120$ using the modified generalized liquid drop model with a Q -value-dependent preformation factor. We have considered only those cluster emissions with half-life below the measurable limits. We have also estimated the probable heavy cluster emitted from each isotope of $^{290-304}120$ with half-life comparable to α -decay half-life and the most probable cluster emission with the least half-life among all cluster-daughter combinations possible, and the predicted decays have either magic number of protons or neutrons or near to it. The highest and second highest α -decay half-life from $^{290-304}120$ corresponds to $^{298}120$ and $^{304}120$, both isotopes with magic or semimagic numbers. Thus, the role of the magic number in stability is highlighted through our paper. The predicted α half-lives are compared with other theoretical models and are in agreement. For the first time we explore the possibility of 2α decay from the superheavy (SH) nuclei. The agreement in theoretical α -decay half-lives with experimental values for the isotopes in the decay chains of $Z = 120$ shows the predictability of the model in the SH region, and so we predict the isotopes $^{290,292}120$ decays by 6α -decay chains and even-even isotopes $^{294-304}120$ decays by 4α -decay chains. Our predictions become particularly important as the predicted half-lives are within experimentally measurable limits and can be detected in the near future.

DOI: [10.1103/PhysRevC.105.054605](https://doi.org/10.1103/PhysRevC.105.054605)

I. INTRODUCTION

In recent years, researchers have greater interest for studying the synthesis and decay of superheavy nuclei (SHN) near the predicted region of island of stability. The main aim of these studies is to develop stable nuclei in the SH region and to have detailed understanding of nuclear structure. Up to now, SHN with $Z \leq 118$ has been experimentally synthesized by either cold fusion reaction or hot fusion reaction. Through cold fusion reaction, scientists have successfully synthesized SHE up to $Z = 112$ at GSI [1–6] and SHE with $Z = 113$ at the RIKEN (Japan) laboratory [7]. Researchers at the Joint Institute for Nuclear Research-Flerov Laboratory of Nuclear Reactions (Dubna) laboratory synthesized elements with $Z = 112-116, 118$ through the hot fusion process [8–13]. In 2011 Oganessian *et al.* [14] synthesized isotopes of $Z = 117$ in the fusion reaction of the radioactive target nuclei ^{249}Bk and the doubly magic ^{48}Ca ions. Several experimental attempts to synthesize isotopes $Z = 119$ and $Z = 120$ was performed in the laboratories using the reactions $^{50}\text{Ti} + ^{249}\text{Bk}$ [15], $^{58}\text{Fe} + ^{244}\text{Pu}$ [16], and $^{54}\text{Cr} + ^{248}\text{Cm}$ [17]. In an attempt to produce the new element $Z = 120$, Hofmann *et al.* [17] investigated the reaction $^{54}\text{Cr} + ^{248}\text{Cm}$ with the aim to study the production and decay properties of isotopes of element $Z = 120$. The effort to produce new elements needs a strong theoretical support that could be helpful to experimentalists in planning their work.

SHN with $Z = 120$ is of great interest among researchers as it is an element with a predicted magic number of protons. Therefore, researchers have performed numerous theoretical studies and predictions on this element. Gherghescu and Carjan [18] studied the two and three fragment decay from $Z = 120$ isotopes using the macroscopic-microscopic method to obtain the total deformation energy. Ahmad *et al.* [19] studied the properties of $Z = 120$ SHN and decay chains of $^{292,304}120$ using relativistic and nonrelativistic formalisms. Santhosh and Priyanka [20] predicted α -decay chains of $^{272-319}120$ using the model Coulomb and proximity potential model (CPPM) for deformed nuclei. Saxena *et al.* [21] developed a new formula for α -decay half-life of $Z = 120$ isotopes.

Many theoretical studies are performed with the intention to study the possible decay chances from SHN. α decay and spontaneous fission (SF) are the decay process experimentally observed in SHN so far. Several experimental and theoretical studies on the cluster radioactivity in the trans-lead region leading to stable daughter nuclei have been done [22–25]. In 2011, Poenaru *et al.* [26] proposed the concept of heavy particle radioactivity (HPR) which allows the emission of emitted particles with $Z_C > 28$ from parents with $Z > 110$ thereby predicting the possibility where HPR is stronger than α decay in SHN. Poenaru *et al.* [27,28] then developed a universal curve for α decay and cluster radioactivity based on fission approach. Karpov *et al.* [29] studied the decay properties and stability of heavy nuclei with $Z \leq 132$. In the present paper, we would also like to consider heavy-cluster decay from the SHN with $Z = 120$ using the modified generalized liquid drop

[✉]drkpsanthosh@gmail.com

model (MGLDM) with the Q -value-dependent preformation factor.

Light cluster emission from heavy and SHN are theoretically investigated using various theoretical approaches [30–32]. The emission of even-even light clusters, such as Be, C, O, Ne, Mg, and Si from SHN with $Z = 120$ are recently studied using MGLDM [33]. Among the various approaches by different authors, besides the work performed by Poenaru and co-workers [26,28,34,35], only a few models are found successful in the predictions of heavy-cluster radioactivity in the SHN with half-lives comparable or dominant over α decay. Zhang and Wang [36] using universal decay law (UDL) formula predicts that the cluster radioactivity dominates over α decay for nuclei with $Z \geq 118$, and the isotopes of $^{292-296,308-318}118$, $^{284-304,308-324}120$, and $^{316-322}122$ are the most likely candidates as the heavy-cluster emitters. Another successful model that could predict HPR with half-life comparable to or even dominant over α decay for some of the isotopes with $Z \geq 118$ was Coulomb and proximity potential model for deformed nuclei [37]. Our group [38] also succeeded in predicting heavy-cluster emission from superheavy element with $Z = 118$ (Og) using MGLDM with Q -value-dependent preformation factor with half-lives comparable to α half-lives.

Theoretical studies that predict the existence of new stable isotopes and their half-lives are necessary to conduct novel and precise experiments to detect superheavy nuclei. In this paper our main goal is to study whether long-lived SHN could really exist around the predicted magic number $Z = 120$ and $N = 184$. To validate this, we have considered all cluster-daughter combinations in heavy-cluster emissions for each isotopes of $^{290-304}120$ and computed all heavy-cluster decay half-lives using our MGLDM with the Q -value-dependent preformation factor.

The present paper is organized as follows. In Sec. II, we have summarized the theoretical framework which is used in this paper. Section III contains the results of the calculations and the important discussions based on it. Finally, Sec. IV summarizes the entire paper.

II. THE MODEL MGLDM

In MGLDM, for a deformed nucleus, the macroscopic energy is defined as

$$E = E_V + E_S + E_C + E_R + E_P. \quad (1)$$

Here the terms E_V , E_S , E_C , E_R , and E_P represent the volume, surface, Coulomb, rotational, and proximity energy terms, respectively.

The volume, surface, and Coulomb energies for the pre-scission region are given by

$$E_V = -15.494(1 - 1.8I^2)A, \quad (2)$$

$$E_S = 17.9439(1 - 2.6I^2)A^{2/3}(S/4\pi R_0^2), \quad (3)$$

$$E_C = 0.6e^2(Z^2/R_0) \\ \times 0.5 \int (V(\theta)/V_0)(R(\theta)/R_0)^3 \sin \theta d\theta. \quad (4)$$

Here I is the relative neutron excess and S the surface of the deformed nucleus, $V(\theta)$ is the electrostatic potential at the surface, and V_0 is the surface potential of the sphere.

For the post-scission region,

$$E_V = -15.494[(1 - 1.8I_1^2)A_1 + (1 - 1.8I_2^2)A_2], \quad (5)$$

$$E_S = 17.9439[(1 - 2.6I_1^2)A_1^{2/3} + (1 - 2.6I_2^2)A_2^{2/3}], \quad (6)$$

$$E_C = \frac{0.6e^2Z_1^2}{R_1} + \frac{0.6e^2Z_2^2}{R_2} + \frac{e^2Z_1Z_2}{r}. \quad (7)$$

Here A_i , Z_i , R_i , and I_i are the masses, charges, radii, and relative neutron excess of the fragments, r is the distance between the centers of the fragments,

$$E_p(z) = 4\pi\gamma b \left[\frac{C_1C_2}{(C_1 + C_2)} \right] \Phi\left(\frac{z}{b}\right) \quad (8)$$

is the nuclear proximity potential of Blocki *et al.* [39] with γ as the nuclear surface tension coefficient and Φ as the universal proximity potential [40].

The barrier penetrability P is calculated using

$$P = \exp \left\{ -\frac{2}{\hbar} \int_{R_{in}}^{R_{out}} \sqrt{2B(r)[E(r) - E(\text{sphere})]} dr \right\}, \quad (9)$$

where $R_{in} = R_1 + R_2$, $B(r) = \mu$ and $R_{out} = e^2Z_1Z_2/Q$. R_1 and R_2 are the radius of the daughter nuclei and emitted cluster, respectively, μ is the reduced mass, and Q is the released energy.

The partial half-life is related to the decay constant λ by

$$T_{1/2} = \left(\frac{\ln 2}{\lambda} \right) = \left(\frac{\ln 2}{vP_C P} \right). \quad (10)$$

The assault frequency v has been taken as 10^{20} s⁻¹, and the preformation factor [41] is given as

$$P_C = 10^{aQ+bQ^2+c}, \quad (11)$$

with $a = -0.25736$, $b = 6.37291 \times 10^{-4}$, and $c = 3.35106$.

III. RESULTS AND DISCUSSION

In the present paper, we have investigated all probable chances of emission like α decay, cluster decay, and spontaneous fission from even-even superheavy nuclei with atomic number 120 and mass number in the range of $290 \leq A \leq 304$. We have considered all possible cluster-daughter combinations for each isotope of $^{290-304}120$, and the heavy-cluster half-lives are calculated using our MGLDM with the Q -value-dependent preformation factor. MGLDM is a well-proved theoretical model by Santhosh and Jose [41] where the GLDM of Royer and Reinaud [42,43] is modified by adding proximity potential developed by Blocki *et al.* [39].

The decay energy or the Q value of the reaction is calculated using the expression,

$$Q = \Delta M_p - (\Delta M_d + \Delta M_c). \quad (12)$$

Here ΔM_p , ΔM_d , and ΔM_c are the masses of parent, daughter nuclei, and cluster, respectively. Any small uncertainty in the Q value will induce a large error in the predicted

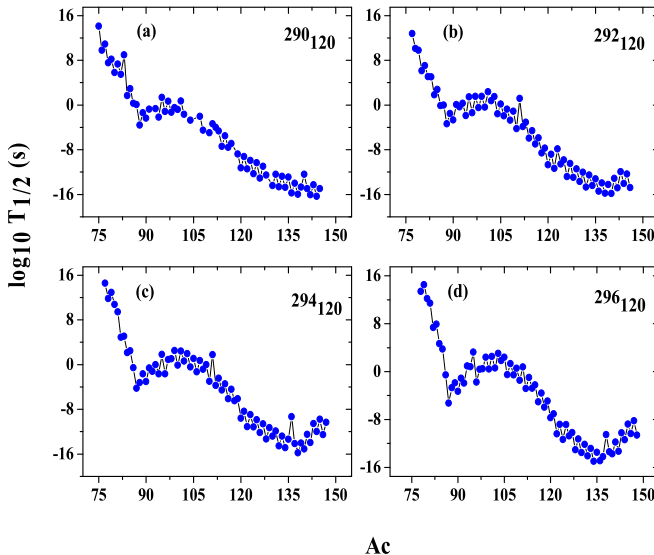


FIG. 1. The variation of the logarithm of probable heavy-cluster decay half-life in seconds vs cluster size for the isotopes $^{290,292,294,296}120$.

half-life. We rely on the masses from the latest mass evaluation table [44] in order to calculate the Q value, and for those nuclei whose experimental values are not available are taken from KTUY05 [45].

One of the important goals of our paper is to identify long-lived SHN near the predicted island of stability and estimates the modes of decay. From the possible fragment cluster combinations for each parent isotope $^{290-304}120$, we have chosen only those heavy-cluster emissions that meet the following criteria: With half-life of cluster emission (up to 10^{30} s) and branching ratio relative to α decay (down to 10^{-19}) which are within the experimentally measurable limit. The branching ratio is calculated using the expression,

$$b = \frac{\lambda_{\text{cluster}}}{\lambda_{\alpha}} = \frac{T_{1/2}^{\alpha}}{T_{1/2}^{\text{cluster}}}, \quad (13)$$

where λ_{cluster} and λ_{α} are the decay constant in cluster emission and α decay, respectively, from parent SHN. $T_{1/2}^{\alpha}$ and $T_{1/2}^{\text{cluster}}$ are the α -decay half-life and the cluster decay half-life, respectively.

The graph with cluster size along the X axis and logarithm of half-life along the Y axis for the $^{290,292,294,296}120$ parent isotope are shown in Figs. 1(a)–1(d). Similar graphs in the case of $^{298,300,302,304}120$ are shown in Figs. 2(a)–2(d). All the graph shows similar behavior with half-life shows a decreasing trend as cluster size increases. All probable heavy cluster decay in the case of even-even isotopes of $^{290-304}120$ within the experimental limit is shown in Tables I–IV. Columns 1–4 represent the parent nuclei, probable heavy cluster, daughter nuclei, and Q value, respectively. Column 5 denotes the half-life in seconds for the heavy-cluster emission. The α half-lives given in these tables are computed using MGLDM. There are many HPRs possible from SHN with $Z = 120$, such as Ge, Se, Ga, Br, Kr, Rb, Sr, Y, Zr, Nb, Mo, Tc, Ru, Rb, Pd, Ag, Cd, In, Sn, Ce (cerium), Sb, Te (tellurium), I, Xe

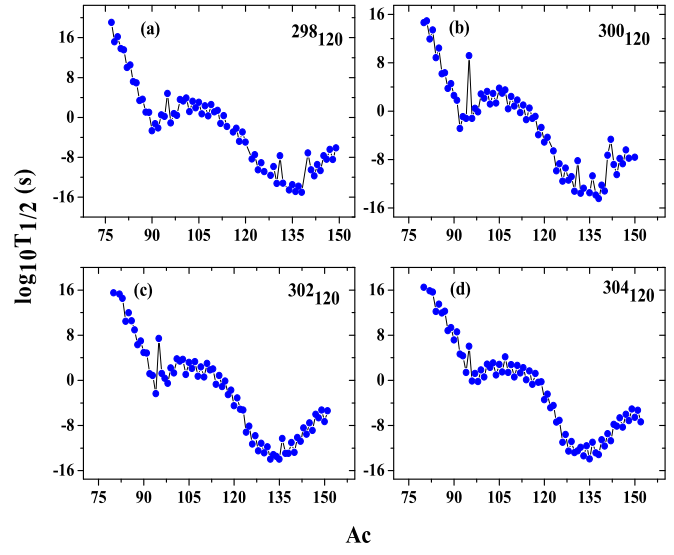


FIG. 2. The variation of the logarithm of probable heavy-cluster decay half-life in seconds vs cluster size for the isotopes $^{298,300,302,304}120$.

(xenon), Cs, Ba (barium), and La as shown in Tables I–IV. Among this, chances of emission, such as Ge, Se, Ga, Br, Sr, and Kr from SHN are predicted by Poenaru *et al.* [26]. All the heavy clusters predicted in Tables I–IV with half-life within experimentally measurable limit are with $Z_C \geq 32$. Our predictions are in agreement with the concept of the HPR by Poenaru *et al.* [26] where the emissions of heavy clusters with $Z_C > 28$ occurs from SHN with $Z > 110$.

One of the prominent decay modes in SHN is α decay. Table V denotes the chances of cluster emissions from each isotope of $^{290-304}120$ with half-life comparable to that of α -decay half-life. Columns 1–4 denote the parent nuclei, probable cluster, daughter nuclei, and Q value, respectively. Columns 5 and 6 represent the heavy-cluster half-life and α decay half-life from each isotope of $^{290-304}120$. The last column denotes the branching ratio of predicted heavy cluster with respect to α decay. From the predicted α half-life, it is noted that the isotope $^{298}120$ has the highest α -decay half-life compared to other isotopes, and so we can conclude that this isotope is more stable than other isotopes with $Z = 120$. The second highest α half-life corresponds to the isotope $^{304}120$, which is doubly magic in nature ($Z = 120$ and $N = 184$). These findings increase the scope for the search of long-lived neutron-rich SHN in laboratories. The extra stability of neutron numbers $N = 178$ and 194 in the SH region is highlighted by Santhosh and Sukumaran [46]. Wang *et al.* [47] suggests that for SHN $Z = 116, 117$, and 118, the smallest α -decay energy occurs at $N = 178$ instead of 184. Siddiqui *et al.* [48] predicts $N = 168, 174$, and 178 as deformed neutron-magic numbers for the SHN with $Z = 122$ and 128. These publications support our findings that $N = 178$ shows the semimagic nature for SHN.

Poenaru *et al.* [26] suggest that the concepts of HPR permits the spontaneous emission of the heavy particle with a larger atomic number $Z_C > 28$ from SHN with $Z > 110$.

TABLE I. The predicted half-lives for various clusters probable from SHN $^{290,292}120$.

Parent nuclei, $^{290}120$				Parent nuclei, $^{292}120$			
Emitted cluster	Daughter nuclei	Q value (MeV)	$T_{1/2}$ (s)	Emitted cluster	Daughter nuclei	Q value (MeV)	$T_{1/2}$ (s)
^4He	^{286}Og	12.8351	1.23×10^{-05}	^4He	^{288}Og	12.7151	2.02×10^{-05}
^{74}Ge	^{216}Ra	279.9514	$3.24 \times 10^{+12}$	^8Be	^{284}Lv	24.5283	$1.90 \times 10^{+14}$
^{75}Ga	^{215}Ac	272.2536	$1.29 \times 10^{+14}$	^{77}Ge	^{215}Ra	278.5589	$6.04 \times 10^{+12}$
^{76}Ge	^{214}Ra	282.9399	$6.15 \times 10^{+09}$	^{78}Ge	^{214}Ra	281.6490	$1.32 \times 10^{+10}$
^{77}Ge	^{213}Ra	281.3360	$8.00 \times 10^{+10}$	^{79}As	^{213}Fr	287.0690	$6.38 \times 10^{+09}$
^{78}Se	^{212}Rn	295.5059	$3.69 \times 10^{+07}$	^{80}Se	^{212}Rn	296.2995	$1.41 \times 10^{+06}$
^{79}Se	^{211}Rn	294.4925	$1.61 \times 10^{+08}$	^{81}Se	^{211}Rn	295.0240	$1.07 \times 10^{+07}$
^{80}Se	^{210}Rn	297.1845	$6.22 \times 10^{+05}$	^{82}Se	^{210}Rn	297.0789	$1.21 \times 10^{+05}$
^{81}Se	^{209}Rn	295.1500	$2.02 \times 10^{+07}$	^{83}Br	^{209}At	301.7770	$1.03 \times 10^{+05}$
^{82}Se	^{208}Rn	297.0699	$3.13 \times 10^{+05}$	^{84}Kr	^{208}Po	309.7889	$6.86 \times 10^{+01}$
^{83}Br	^{207}At	297.4690	$9.88 \times 10^{+08}$	^{85}Kr	^{207}Po	308.5063	$6.00 \times 10^{+02}$
^{84}Kr	^{206}Po	310.4483	$4.83 \times 10^{+01}$	^{86}Kr	^{206}Po	311.3347	7.98×10^{-01}
^{85}Kr	^{205}Po	308.8213	$8.53 \times 10^{+02}$	^{87}Rb	^{205}Bi	315.5428	9.33×10^{-01}
^{86}Kr	^{204}Po	311.4267	$2.04 \times 10^{+00}$	^{88}Sr	^{204}Pb	322.9115	4.55×10^{-04}
^{87}Rb	^{203}Bi	315.9428	$1.18 \times 10^{+00}$	^{89}Sr	^{203}Pb	320.8760	3.12×10^{-02}
^{88}Sr	^{202}Pb	323.6826	2.54×10^{-04}	^{90}Sr	^{202}Pb	321.7691	2.17×10^{-03}
^{89}Sr	^{201}Pb	321.3000	$5.16 \times 10^{+02}$	^{91}Sr	^{201}Pb	318.8030	$1.16 \times 10^{+00}$
^{90}Sr	^{200}Pb	322.0191	4.28×10^{-03}	^{92}Sr	^{200}Pb	318.9980	4.67×10^{-01}
^{91}Y	^{199}Tl	324.2303	1.74×10^{-01}	^{93}Y	^{199}Tl	322.1660	$1.96 \times 10^{+00}$
^{93}Zr	^{197}Hg	327.4820	2.34×10^{-01}	^{94}Zr	^{198}Hg	328.1036	1.25×10^{-02}
^{94}Zr	^{196}Hg	328.9152	6.71×10^{-03}	^{95}Nb	^{197}Au	327.8060	$2.87 \times 10^{+01}$
^{95}Nb	^{195}Au	328.4322	1.95×10^{-02}	^{96}Zr	^{196}Hg	327.1448	4.29×10^{-02}
^{96}Zr	^{194}Hg	327.4428	7.18×10^{-02}	^{97}Zr	^{195}Hg	323.8357	$3.38 \times 10^{+01}$
^{97}Nb	^{193}Au	328.8310	$4.98 \times 10^{+00}$	^{98}Mo	^{194}Pt	332.7561	$7.12 \times 10^{+05}$
^{98}Mo	^{192}Pt	334.2245	4.98×10^{-02}	^{99}Mo	^{193}Pt	330.3297	$3.66 \times 10^{+01}$
^{99}Mo	^{191}Pt	333.1434	3.35×10^{-01}	^{100}Mo	^{192}Pt	332.3615	3.98×10^{-01}
^{100}Mo	^{190}Pt	333.3195	1.63×10^{-01}	^{101}Mo	^{191}Pt	329.0979	$2.36 \times 10^{+02}$
^{101}Tc	^{189}Ir	334.6150	$5.31 \times 10^{+00}$	^{102}Mo	^{190}Pt	330.7525	$5.89 \times 10^{+00}$
^{102}Ru	^{188}Os	340.0636	2.22×10^{-02}	^{103}Tc	^{189}Ir	332.9340	$3.04 \times 10^{+01}$
^{104}Ru	^{186}Os	340.9156	1.89×10^{-03}	^{104}Ru	^{188}Os	339.1129	2.74×10^{-02}
^{107}Rh	^{183}Re	342.4940	9.56×10^{-03}	^{105}Ru	^{187}Os	337.0334	$1.55 \times 10^{+00}$
^{108}Pd	^{182}W	347.5903	3.21×10^{-05}	^{106}Ru	^{186}Os	339.2029	1.20×10^{-02}
^{110}Pd	^{180}W	347.7870	1.12×10^{-05}	^{107}Rh	^{185}Re	340.5630	1.72×10^{-01}
^{111}Ag	^{179}Ta	348.3927	4.34×10^{-04}	^{108}Pd	^{184}W	345.1096	2.01×10^{-03}
^{112}Pd	^{178}W	346.5490	9.92×10^{-05}	^{109}Rh	^{183}Re	340.6890	7.64×10^{-02}
^{113}Cd	^{177}Hf	351.7439	2.20×10^{-05}	^{110}Pd	^{182}W	346.4570	6.00×10^{-05}
^{114}Cd	^{176}Hf	354.4112	4.19×10^{-08}	^{111}Pd	^{181}W	340.4178	$1.57 \times 10^{+01}$
^{115}Cd	^{175}Hf	352.3862	3.21×10^{-06}	^{112}Pd	^{180}W	345.8381	1.33×10^{-04}
^{116}Cd	^{174}Hf	354.3770	2.57×10^{-08}	^{113}Ag	^{179}Ta	347.2643	8.55×10^{-04}
^{117}In	^{173}Lu	355.6439	1.29×10^{-07}	^{114}Cd	^{178}Hf	352.3301	1.25×10^{-06}
^{119}Sn	^{171}Yb	359.1918	1.65×10^{-09}	^{115}Cd	^{177}Hf	350.8451	2.64×10^{-05}
^{120}Sn	^{170}Yb	361.6823	5.53×10^{-12}	^{116}Cd	^{176}Hf	353.1688	1.04×10^{-07}
^{121}Sn	^{169}Yb	359.3949	6.20×10^{-10}	^{117}In	^{175}Lu	353.9886	1.39×10^{-06}
^{122}Sn	^{168}Yb	361.3432	3.75×10^{-12}	^{118}Sn	^{174}Yb	358.4774	2.62×10^{-09}
^{123}Sb	^{167}Tm	361.5877	1.27×10^{-10}	^{119}Sn	^{173}Yb	357.4962	2.03×10^{-08}
^{124}Te	^{166}Er	365.2713	5.21×10^{-13}	^{120}Sn	^{172}Yb	360.2338	2.03×10^{-11}
^{125}Te	^{165}Er	363.3646	4.70×10^{-11}	^{121}Sn	^{171}Yb	358.3841	1.52×10^{-09}
^{126}Te	^{164}Er	365.8282	8.19×10^{-14}	^{122}Sn	^{170}Yb	360.5852	4.69×10^{-12}
^{127}I	^{163}Ho	365.1823	1.05×10^{-11}	^{123}Sb	^{169}Tm	358.9714	1.38×10^{-08}
^{128}Te	^{162}Er	365.1482	2.99×10^{-13}	^{124}Sn	^{168}Yb	359.6961	2.77×10^{-11}
^{130}Xe	^{160}Dy	369.3732	4.00×10^{-15}	^{125}Sb	^{167}Tm	360.6799	1.52×10^{-10}
^{131}Xe	^{159}Dy	367.4007	4.12×10^{-13}	^{126}Te	^{166}Er	364.8713	1.58×10^{-13}
^{132}Xe	^{158}Dy	369.5063	2.28×10^{-15}	^{127}Te	^{165}Er	362.6833	3.28×10^{-11}
^{133}Cs	^{157}Tb	368.6543	1.68×10^{-13}	^{128}Te	^{164}Er	364.8166	1.17×10^{-13}
^{134}Ba	^{156}Gd	371.3048	1.80×10^{-15}	^{129}I	^{163}Ho	364.7653	3.79×10^{-12}

TABLE I. (*Continued.*)

Parent nuclei, $^{290}120$				Parent nuclei, $^{292}120$			
Emitted cluster	Daughter nuclei	Q value (MeV)	$T_{1/2}$ (s)	Emitted cluster	Daughter nuclei	Q value (MeV)	$T_{1/2}$ (s)
^{135}Cs	^{155}Tb	368.6516	1.33×10^{-13}	^{130}Xe	^{162}Dy	367.9420	2.16×10^{-14}
^{136}Ba	^{154}Gd	372.4129	1.66×10^{-11}	^{131}Xe	^{161}Dy	366.3494	9.98×10^{-13}
^{137}Ba	^{153}Gd	370.4238	1.04×10^{-14}	^{132}Xe	^{160}Dy	368.8317	2.19×10^{-15}
^{138}Ba	^{152}Gd	372.7885	1.03×10^{-16}	^{133}Xe	^{159}Dy	366.6907	3.08×10^{-13}
^{139}La	^{151}Eu	371.6991	1.98×10^{-15}	^{134}Xe	^{158}Dy	368.4131	4.02×10^{-15}
^{140}Ba	^{150}Gd	368.8530	4.17×10^{-13}	^{135}Cs	^{157}Tb	368.2250	6.29×10^{-14}

TABLE II. The predicted half-lives for various clusters probable from SHN $^{294,296}120$.

Parent nuclei, $^{294}120$				Parent nuclei, $^{296}120$			
Emitted cluster	Daughter nuclei	Q value (MeV)	$T_{1/2}$ (s)	Emitted cluster	Daughter nuclei	Q value (MeV)	$T_{1/2}$ (s)
^4He	^{290}Og	12.4951	5.49×10^{-05}	^4He	^{292}Og	12.2251	5.42×10^{-04}
^{77}Ge	^{217}Ra	275.8729	$3.85 \times 10^{+14}$	^{78}Ge	^{218}Ra	276.7810	$2.35 \times 10^{+13}$
^{78}Ge	^{216}Ra	279.1210	$6.66 \times 10^{+11}$	^{79}Ge	^{217}Ra	275.2100	$3.05 \times 10^{+14}$
^{79}Ge	^{215}Ra	277.5460	$8.61 \times 10^{+12}$	^{80}Ge	^{216}Ra	277.8143	$1.63 \times 10^{+12}$
^{80}Ge	^{214}Ra	279.9923	$5.93 \times 10^{+10}$	^{81}As	^{215}Fr	283.7853	$2.75 \times 10^{+11}$
^{81}As	^{213}Fr	286.6363	$2.82 \times 10^{+09}$	^{82}Se	^{214}Rn	293.4839	$2.39 \times 10^{+07}$
^{82}Se	^{212}Rn	296.8039	$8.24 \times 10^{+04}$	^{83}Se	^{213}Rn	292.6070	$8.63 \times 10^{+07}$
^{83}Br	^{211}At	301.2113	$1.25 \times 10^{+05}$	^{84}Se	^{212}Rn	296.1777	$4.40 \times 10^{+04}$
^{84}Kr	^{210}Po	308.9424	$1.46 \times 10^{+02}$	^{85}Br	^{211}At	301.7923	$5.94 \times 10^{+03}$
^{85}Kr	^{209}Po	308.3964	$2.77 \times 10^{+02}$	^{86}Kr	^{210}Po	310.7888	2.75×10^{-01}
^{86}Kr	^{208}Po	311.2853	2.77×10^{-01}	^{87}Rb	^{209}Bi	314.4265	5.62×10^{-06}
^{87}Rb	^{207}Bi	318.9334	6.10×10^{-05}	^{88}Sr	^{208}Pb	321.2402	2.11×10^{-03}
^{88}Sr	^{206}Pb	322.2572	6.22×10^{-04}	^{89}Sr	^{207}Pb	320.2310	1.29×10^{-02}
^{89}Sr	^{205}Pb	320.5292	2.12×10^{-02}	^{90}Sr	^{206}Pb	321.3037	4.98×10^{-04}
^{90}Sr	^{204}Pb	321.6080	8.75×10^{-04}	^{91}Sr	^{205}Pb	318.9922	7.66×10^{-02}
^{91}Sr	^{203}Pb	318.9890	2.46×10^{-01}	^{92}Sr	^{204}Pb	319.5469	1.19×10^{-02}
^{92}Sr	^{202}Pb	319.3580	6.35×10^{-02}	^{93}Sr	^{203}Pb	316.4430	$8.76 \times 10^{+00}$
^{93}Y	^{201}Tl	321.9580	$1.02 \times 10^{+00}$	^{94}Sr	^{202}Pb	316.3567	$6.78 \times 10^{+00}$
^{94}Zr	^{200}Hg	327.3226	2.21×10^{-02}	^{95}Nb	^{201}Au	324.7573	$1.75 \times 10^{+03}$
^{95}Nb	^{199}Au	326.8824	$6.69 \times 10^{+01}$	^{96}Zr	^{200}Hg	326.5122	1.68×10^{-02}
^{96}Zr	^{198}Hg	326.9432	2.07×10^{-02}	^{97}Zr	^{199}Hg	324.0588	$2.46 \times 10^{+00}$
^{97}Zr	^{197}Hg	324.0327	$7.68 \times 10^{+00}$	^{98}Zr	^{198}Hg	323.8113	$2.83 \times 10^{+00}$
^{98}Zr	^{196}Hg	323.6629	$1.15 \times 10^{+01}$	^{99}Nb	^{197}Au	325.0447	$2.52 \times 10^{+02}$
^{99}Nb	^{195}Au	325.4520	$3.07 \times 10^{+02}$	^{100}Mo	^{196}Pt	330.4075	$2.70 \times 10^{+00}$
^{100}Mo	^{194}Pt	331.5031	8.03×10^{-01}	^{101}Mo	^{195}Pt	327.8837	$3.51 \times 10^{+02}$
^{101}Mo	^{193}Pt	328.5495	$2.54 \times 10^{+02}$	^{102}Mo	^{194}Pt	329.8961	$4.00 \times 10^{+00}$
^{102}Mo	^{192}Pt	330.4045	$4.08 \times 10^{+00}$	^{103}Mo	^{193}Pt	327.0106	$1.13 \times 10^{+03}$
^{103}Tc	^{191}Ir	331.8628	$9.31 \times 10^{+01}$	^{104}Mo	^{192}Pt	328.2085	$7.19 \times 10^{+01}$
^{104}Ru	^{190}Os	337.3535	3.57×10^{-01}	^{103}Tc	^{191}Ir	330.5688	$2.57 \times 10^{+02}$
^{105}Ru	^{189}Os	335.4712	$1.29 \times 10^{+01}$	^{106}Ru	^{190}Os	336.6008	3.09×10^{-01}
^{106}Ru	^{188}Os	338.0102	4.82×10^{-02}	^{107}Ru	^{189}Os	334.4197	$2.19 \times 10^{+01}$
^{107}Ru	^{187}Os	335.6319	$5.30 \times 10^{+00}$	^{108}Ru	^{188}Os	336.3682	2.80×10^{-01}
^{108}Ru	^{186}Os	337.2109	1.46×10^{-01}	^{109}Rh	^{187}Re	337.7855	$3.46 \times 10^{+00}$
^{109}Rh	^{185}Re	338.9368	9.58×10^{-01}	^{110}Pd	^{186}W	342.4094	3.46×10^{-02}
^{110}Pd	^{184}W	344.5863	1.05×10^{-03}	^{111}Rh	^{185}W	337.2618	$6.16 \times 10^{+00}$
^{111}Pd	^{183}W	339.2196	$6.03 \times 10^{+01}$	^{112}Pd	^{184}W	343.5974	1.54×10^{-03}
^{112}Pd	^{182}W	345.1181	1.85×10^{-04}	^{113}Pd	^{183}W	341.5266	1.03×10^{-01}
^{113}Ag	^{181}Ta	346.0153	3.72×10^{-03}	^{114}Pd	^{182}W	343.3071	1.70×10^{-03}
^{114}Cd	^{180}Hf	350.3442	2.87×10^{-05}	^{115}Ag	^{181}Ta	344.9913	6.18×10^{-03}
^{115}Cd	^{179}Hf	349.0974	3.40×10^{-04}	^{116}Cd	^{180}Hf	350.0618	8.80×10^{-06}
^{116}Cd	^{178}Hf	351.6977	7.93×10^{-07}	^{117}Cd	^{179}Hf	348.4513	2.49×10^{-04}
^{117}Cd	^{177}Hf	349.8490	4.03×10^{-05}	^{118}Cd	^{178}Hf	350.7072	1.18×10^{-06}

TABLE II. (*Continued.*)

Parent nuclei, $^{294}120$				Parent nuclei, $^{296}120$			
Emitted cluster	Daughter nuclei	Q value (MeV)	$T_{1/2}$ (s)	Emitted cluster	Daughter nuclei	Q value (MeV)	$T_{1/2}$ (s)
^{118}Cd	^{176}Hf	351.8283	3.43×10^{-07}	^{119}In	^{177}Lu	351.6528	1.16×10^{-05}
^{119}In	^{175}Lu	353.4146	8.10×10^{-07}	^{120}Sn	^{176}Yb	356.1597	2.07×10^{-08}
^{120}Sn	^{174}Yb	358.5929	2.51×10^{-10}	^{121}Sn	^{175}Yb	355.4629	8.39×10^{-08}
^{121}Sn	^{173}Yb	357.2985	4.58×10^{-09}	^{122}Sn	^{174}Yb	358.4558	4.00×10^{-11}
^{122}Sn	^{172}Yb	359.7467	7.44×10^{-12}	^{123}Sn	^{173}Yb	356.9374	1.47×10^{-09}
^{123}Sn	^{171}Yb	357.6730	1.13×10^{-09}	^{124}Sn	^{172}Yb	359.0596	4.53×10^{-12}
^{124}Sn	^{170}Yb	359.5481	7.19×10^{-12}	^{125}Sn	^{171}Yb	356.7732	1.37×10^{-09}
^{125}Sb	^{169}Tm	360.0815	1.33×10^{-10}	^{126}Sn	^{170}Yb	358.3489	1.79×10^{-11}
^{126}Te	^{168}Er	363.6065	7.06×10^{-13}	^{127}Sb	^{169}Tm	359.5442	6.37×10^{-11}
^{127}Te	^{167}Er	362.1229	2.54×10^{-11}	^{128}Te	^{168}Er	363.5549	8.78×10^{-14}
^{128}Te	^{166}Er	364.4697	4.96×10^{-14}	^{129}Te	^{167}Er	361.8660	5.85×10^{-12}
^{129}I	^{165}Ho	363.9560	5.31×10^{-12}	^{130}Te	^{166}Er	363.8489	2.92×10^{-14}
^{130}Te	^{164}Er	363.8458	1.56×10^{-13}	^{131}I	^{165}Ho	363.9117	7.00×10^{-13}
^{131}I	^{163}Ho	364.3710	1.26×10^{-12}	^{132}Xe	^{164}Dy	366.8170	8.31×10^{-15}
^{132}Xe	^{162}Dy	368.0105	2.89×10^{-15}	^{133}Xe	^{163}Dy	365.5948	1.40×10^{-13}
^{133}Xe	^{161}Dy	366.2494	1.57×10^{-13}	^{134}Xe	^{162}Dy	367.8773	1.10×10^{-15}
^{134}Xe	^{160}Dy	368.3485	1.31×10^{-15}	^{135}Xe	^{161}Dy	366.0388	3.25×10^{-14}
^{135}Cs	^{159}Tb	367.6640	4.24×10^{-14}	^{136}Xe	^{160}Dy	367.6719	1.26×10^{-15}
^{136}Ba	^{158}Gd	364.6869	4.81×10^{-10}	^{137}Cs	^{159}Tb	367.6480	6.12×10^{-15}
^{137}Ba	^{157}Gd	369.0947	7.51×10^{-15}	^{138}Ba	^{158}Gd	365.0816	2.95×10^{-11}
^{138}Ba	^{156}Gd	371.3465	1.58×10^{-16}	^{139}La	^{157}Gd	368.2552	4.12×10^{-14}

TABLE III. The predicted half-lives for various clusters probable from SHN $^{298,300}120$.

Parent nuclei, $^{298}120$				Parent nuclei, $^{300}120$			
Emitted cluster	Daughter nuclei	Q value (MeV)	$T_{1/2}$ (s)	Emitted cluster	Daughter nuclei	Q value (MeV)	$T_{1/2}$ (s)
^4He	^{294}Og	10.6751	$1.28 \times 10^{+00}$	^4He	^{296}Og	11.8851	1.01×10^{-03}
^{77}Ga	^{221}Ac	264.0323	$1.19 \times 10^{+19}$	^{80}Ge	^{220}Ra	274.0453	$4.12 \times 10^{+14}$
^{78}Ge	^{220}Ra	274.1520	$1.43 \times 10^{+15}$	^{81}As	^{219}Fr	278.6953	$8.01 \times 10^{+14}$
^{79}Ge	^{219}Ra	272.6960	$1.52 \times 10^{+16}$	^{82}Se	^{218}Rn	287.1566	$7.93 \times 10^{+11}$
^{80}Ge	^{218}Ra	275.4443	$6.42 \times 10^{+13}$	^{83}As	^{217}Fr	280.1343	$2.73 \times 10^{+13}$
^{81}As	^{217}Fr	280.7783	$3.52 \times 10^{+13}$	^{84}Se	^{216}Rn	290.4747	$6.59 \times 10^{+08}$
^{82}Se	^{216}Rn	289.9009	$9.94 \times 10^{+09}$	^{85}Se	^{215}Rn	288.3626	$2.69 \times 10^{+10}$
^{83}Se	^{215}Rn	289.0700	$3.30 \times 10^{+10}$	^{86}Kr	^{214}Po	302.5157	$1.52 \times 10^{+06}$
^{84}Se	^{214}Rn	292.8277	$1.54 \times 10^{+07}$	^{87}Kr	^{213}Po	302.1435	$2.12 \times 10^{+06}$
^{85}Br	^{213}At	297.7150	$8.69 \times 10^{+06}$	^{88}Kr	^{212}Po	304.8408	$5.85 \times 10^{+03}$
^{86}Kr	^{212}Po	306.1952	$2.32 \times 10^{+03}$	^{89}Kr	^{211}Po	303.7484	$3.62 \times 10^{+04}$
^{87}Kr	^{211}Po	305.7021	$4.04 \times 10^{+03}$	^{90}Kr	^{210}Po	305.6923	$3.75 \times 10^{+02}$
^{88}Kr	^{210}Po	308.2044	$1.12 \times 10^{+01}$	^{91}Rb	^{209}Bi	310.7837	$6.37 \times 10^{+01}$
^{89}Rb	^{209}Bi	312.5307	$9.62 \times 10^{+00}$	^{92}Sr	^{208}Pb	319.3956	1.31×10^{-03}
^{90}Sr	^{208}Pb	320.2567	1.92×10^{-03}	^{93}Sr	^{207}Pb	317.3180	1.27×10^{-01}
^{91}Sr	^{207}Pb	318.6640	5.07×10^{-02}	^{94}Sr	^{206}Pb	317.4113	5.95×10^{-02}
^{92}Sr	^{206}Pb	319.2126	7.67×10^{-03}	^{95}Rb	^{205}Bi	301.7360	$1.46 \times 10^{+09}$
^{93}Sr	^{205}Pb	316.4162	$3.12 \times 10^{+00}$	^{96}Zr	^{204}Hg	324.9090	6.30×10^{-02}
^{94}Sr	^{204}Pb	316.5156	$1.56 \times 10^{+00}$	^{97}Zr	^{203}Hg	322.9920	$2.83 \times 10^{+00}$
^{95}Nb	^{203}Au	322.4893	$5.94 \times 10^{+04}$	^{98}Zr	^{202}Hg	323.4123	7.46×10^{-01}
^{96}Zr	^{202}Hg	325.3442	7.38×10^{-02}	^{99}Zr	^{201}Hg	320.0635	$6.59 \times 10^{+02}$
^{97}Zr	^{201}Hg	323.1652	$5.67 \times 10^{+00}$	^{100}Zr	^{200}Hg	320.6603	$1.32 \times 10^{+02}$
^{98}Zr	^{200}Hg	323.3503	$2.56 \times 10^{+00}$	^{101}Nb	^{199}Au	322.7647	$1.85 \times 10^{+03}$
^{99}Zr	^{199}Hg	319.7271	$3.61 \times 10^{+03}$	^{102}Mo	^{198}Pt	328.2500	$1.51 \times 10^{+01}$
^{100}Zr	^{198}Hg	319.8913	$1.85 \times 10^{+03}$	^{103}Mo	^{197}Pt	326.1607	$8.37 \times 10^{+02}$

TABLE III. (*Continued.*)

Parent nuclei, $^{298}120$				Parent nuclei, $^{300}120$			
Emitted cluster	Daughter nuclei	Q value (MeV)	$T_{1/2}$ (s)	Emitted cluster	Daughter nuclei	Q value (MeV)	$T_{1/2}$ (s)
^{101}Nb	^{197}Au	322.5907	$7.20 \times 10^{+03}$	^{104}Mo	^{196}Pt	327.7745	$2.13 \times 10^{+01}$
^{102}Mo	^{196}Pt	328.7705	$1.45 \times 10^{+01}$	^{105}Mo	^{195}Pt	324.9108	$6.05 \times 10^{+03}$
^{103}Mo	^{195}Pt	326.3148	$1.68 \times 10^{+03}$	^{106}Mo	^{194}Pt	325.6751	$9.40 \times 10^{+02}$
^{104}Mo	^{194}Pt	327.6701	$7.64 \times 10^{+01}$	^{107}Tc	^{193}Ir	328.0662	$3.15 \times 10^{+03}$
^{105}Tc	^{193}Ir	329.3862	$1.02 \times 10^{+03}$	^{108}Ru	^{192}Os	334.3232	$3.53 \times 10^{+07}$
^{106}Ru	^{192}Os	334.7652	$4.87 \times 10^{+00}$	^{109}Ru	^{191}Os	331.9132	$3.65 \times 10^{+09}$
^{107}Ru	^{191}Os	332.8182	$2.04 \times 10^{+02}$	^{110}Ru	^{190}Os	333.5608	$6.65 \times 10^{+00}$
^{108}Ru	^{190}Os	334.9288	$1.93 \times 10^{+00}$	^{111}Rh	^{189}Re	335.0630	$6.77 \times 10^{+01}$
^{109}Ru	^{189}Os	332.2847	$3.61 \times 10^{+02}$	^{112}Pd	^{188}W	339.7700	5.69×10^{-01}
^{110}Ru	^{188}Os	333.7702	$1.28 \times 10^{+01}$	^{113}Pd	^{187}W	338.2750	$1.02 \times 10^{+01}$
^{111}Rh	^{187}Re	336.0805	$2.40 \times 10^{+01}$	^{114}Pd	^{186}W	340.7795	3.90×10^{-02}
^{112}Pd	^{186}W	341.3905	5.61×10^{-02}	^{115}Pd	^{185}W	338.5938	$3.27 \times 10^{+00}$
^{113}Pd	^{185}W	339.5388	$2.19 \times 10^{+00}$	^{116}Pd	^{184}W	340.3174	6.43×10^{-02}
^{114}Pd	^{184}W	341.7564	1.51×10^{-02}	^{117}Ag	^{181}Ta	342.2548	1.32×10^{-01}
^{116}Cd	^{182}Hf	347.3225	1.10×10^{-03}	^{118}Cd	^{182}Hf	347.5320	1.23×10^{-04}
^{117}Cd	^{181}Hf	346.3812	6.64×10^{-03}	^{119}Cd	^{181}Hf	346.1628	2.03×10^{-03}
^{118}Cd	^{180}Hf	349.0413	1.44×10^{-05}	^{120}Cd	^{180}Hf	348.5163	7.77×10^{-06}
^{119}Cd	^{179}Hf	347.0029	1.09×10^{-03}	^{121}In	^{179}Lu	349.6750	4.72×10^{-05}
^{120}Cd	^{178}Hf	348.9522	1.08×10^{-05}	^{123}Sn	^{177}Yb	353.5826	2.65×10^{-07}
^{122}Sn	^{176}Yb	355.9926	4.26×10^{-09}	^{124}Sn	^{176}Yb	356.5055	1.37×10^{-10}
^{123}Sn	^{175}Yb	355.0718	3.14×10^{-08}	^{125}Sn	^{175}Yb	355.3720	2.01×10^{-09}
^{124}Sn	^{174}Yb	357.7387	2.76×10^{-11}	^{126}Sn	^{174}Yb	357.7395	2.57×10^{-12}
^{125}Sn	^{173}Yb	356.0076	7.59×10^{-10}	^{127}Sn	^{173}Yb	355.8022	4.01×10^{-10}
^{126}Sn	^{172}Yb	357.8304	1.23×10^{-11}	^{128}Sn	^{172}Yb	357.3974	3.80×10^{-12}
^{128}Te	^{170}Er	361.6624	2.17×10^{-12}	^{129}Sb	^{171}Tm	358.6193	1.47×10^{-11}
^{129}Sb	^{169}Tm	358.4642	1.26×10^{-10}	^{130}Te	^{170}Er	362.2416	5.45×10^{-14}
^{130}Te	^{168}Er	362.9041	5.41×10^{-14}	^{131}Te	^{169}Er	357.6845	6.23×10^{-09}
^{131}Te	^{167}Er	357.8326	1.99×10^{-08}	^{132}Te	^{168}Er	362.9592	2.73×10^{-14}
^{132}Te	^{166}Er	362.6740	6.32×10^{-14}	^{133}I	^{167}Ho	362.9190	1.76×10^{-13}
^{134}Xe	^{164}Dy	366.6538	2.64×10^{-15}	^{135}I	^{165}Ho	363.4581	3.23×10^{-14}
^{135}Xe	^{163}Dy	365.3542	3.14×10^{-14}	^{136}Cs	^{164}Tb	363.1987	1.88×10^{-11}
^{136}Xe	^{162}Dy	367.1707	1.25×10^{-15}	^{137}Cs	^{163}Tb	365.9216	1.33×10^{-14}
^{137}Cs	^{161}Tb	366.5672	1.47×10^{-14}	^{138}Ba	^{162}Gd	367.3216	3.40×10^{-15}
^{138}Ba	^{160}Gd	368.7633	8.92×10^{-16}	^{139}Ba	^{161}Gd	365.1996	5.74×10^{-13}
^{140}Ba	^{158}Gd	361.0790	7.39×10^{-08}	^{140}Ba	^{160}Gd	365.9907	6.15×10^{-14}
^{141}La	^{157}Gd	364.9510	2.77×10^{-11}	^{141}Ba	^{159}Gd	360.5560	5.20×10^{-08}

TABLE IV. The predicted half-lives for various clusters probable from SHN $^{302,304}120$.

Parent nuclei, $^{302}120$				Parent nuclei, $^{304}120$			
Emitted cluster	Daughter nuclei	Q value (MeV)	$T_{1/2}$ (s)	Emitted cluster	Daughter nuclei	Q value (MeV)	$T_{1/2}$ (s)
^4He	^{298}Og	11.7951	1.52×10^{-03}	^4He	^{300}Og	11.5151	6.65×10^{-03}
^{80}Ge	^{222}Ra	272.5753	$3.05 \times 10^{+15}$	^{80}Ge	^{224}Ra	270.9794	$2.91 \times 10^{+16}$
^{82}Ge	^{220}Ra	272.5051	$1.79 \times 10^{+15}$	^{82}Ge	^{222}Ra	271.3651	$7.34 \times 10^{+15}$
^{83}As	^{219}Fr	278.4113	$3.28 \times 10^{+14}$	^{83}As	^{221}Fr	276.6623	$4.20 \times 10^{+15}$
^{84}Se	^{218}Rn	288.0904	$2.90 \times 10^{+10}$	^{84}Se	^{220}Rn	285.6056	$1.52 \times 10^{+12}$
^{85}Se	^{215}Rn	286.1146	$8.96 \times 10^{+11}$	^{85}Se	^{219}Rn	283.8542	$3.05 \times 10^{+13}$
^{86}Se	^{216}Rn	287.6102	$3.50 \times 10^{+10}$	^{86}Se	^{218}Rn	285.5559	$8.30 \times 10^{+11}$
^{87}Kr	^{215}Po	298.6112	$8.87 \times 10^{+08}$	^{87}Br	^{217}At	289.7670	$1.62 \times 10^{+12}$
^{88}Kr	^{214}Po	301.5213	$2.00 \times 10^{+06}$	^{88}Kr	^{216}Po	298.1789	$6.14 \times 10^{+08}$
^{89}Kr	^{213}Po	300.5498	$9.37 \times 10^{+06}$	^{89}Kr	^{215}Po	297.3475	$2.17 \times 10^{+09}$
^{90}Kr	^{212}Po	302.6887	$8.21 \times 10^{+04}$	^{90}Kr	^{214}Po	299.6992	$1.44 \times 10^{+07}$

TABLE IV. (*Continued.*)

Parent nuclei, ^{302}Zr				Parent nuclei, ^{304}Zr			
Emitted cluster	Daughter nuclei	Q value (MeV)	$T_{1/2}$ (s)	Emitted cluster	Daughter nuclei	Q value (MeV)	$T_{1/2}$ (s)
^{91}Rb	^{211}Bi	306.9640	$6.76 \times 10^{+04}$	^{91}Kr	^{213}Po	297.8980	$3.62 \times 10^{+08}$
^{92}Sr	^{210}Pb	314.9555	$1.47 \times 10^{+01}$	^{92}Sr	^{212}Pb	310.6858	$4.28 \times 10^{+04}$
^{93}Sr	^{209}Pb	315.0606	$7.28 \times 10^{+00}$	^{93}Sr	^{211}Pb	310.8489	$2.07 \times 10^{+04}$
^{94}Sr	^{208}Pb	317.9543	4.29×10^{-03}	^{94}Sr	^{210}Pb	313.8442	$2.36 \times 10^{+01}$
^{95}Rb	^{207}Bi	303.3056	$2.57 \times 10^{+07}$	^{95}Rb	^{209}Bi	304.4197	$1.06 \times 10^{+06}$
^{96}Sr	^{206}Pb	314.0696	$1.69 \times 10^{+01}$	^{96}Sr	^{208}Pb	314.9426	7.39×10^{-01}
^{97}Zr	^{205}Hg	322.5907	$2.32 \times 10^{+00}$	^{97}Y	^{207}Ti	317.4250	$1.63 \times 10^{+01}$
^{98}Zr	^{204}Hg	323.3371	2.90×10^{-01}	^{98}Zr	^{206}Hg	322.5030	6.24×10^{-01}
^{99}Zr	^{203}Hg	320.2503	$1.61 \times 10^{+02}$	^{99}Zr	^{205}Hg	320.1790	$6.72 \times 10^{+01}$
^{100}Zr	^{202}Hg	321.0823	$1.87 \times 10^{+01}$	^{100}Zr	^{204}Hg	321.3371	$3.66 \times 10^{+00}$
^{101}Zr	^{201}Hg	318.1885	$6.04 \times 10^{+03}$	^{101}Zr	^{203}Hg	318.7053	$7.48 \times 10^{+02}$
^{102}Zr	^{200}Hg	318.4513	$2.52 \times 10^{+03}$	^{102}Zr	^{202}Hg	319.2033	$1.82 \times 10^{+02}$
^{103}Nb	^{199}Au	321.4827	$5.09 \times 10^{+03}$	^{103}Nb	^{201}Au	321.7000	$1.19 \times 10^{+03}$
^{104}Mo	^{198}Pt	327.6140	$1.03 \times 10^{+01}$	^{104}Mo	^{200}Pt	327.2190	$8.31 \times 10^{+00}$
^{105}Mo	^{197}Pt	325.1167	$1.43 \times 10^{+03}$	^{105}Mo	^{199}Pt	324.9957	$6.68 \times 10^{+02}$
^{106}Mo	^{196}Pt	326.1395	$1.25 \times 10^{+02}$	^{106}Mo	^{198}Pt	326.3090	$3.04 \times 10^{+01}$
^{107}Tc	^{195}Ir	327.8023	$1.96 \times 10^{+03}$	^{107}Mo	^{197}Pt	323.2417	$1.43 \times 10^{+04}$
^{108}Ru	^{194}Os	333.4561	$4.94 \times 10^{+00}$	^{108}Ru	^{196}Os	332.2110	$2.37 \times 10^{+01}$
^{109}Ru	^{193}Os	331.4923	$2.29 \times 10^{+02}$	^{109}Ru	^{195}Os	330.5180	$6.15 \times 10^{+02}$
^{110}Ru	^{192}Os	333.3152	$3.75 \times 10^{+00}$	^{110}Ru	^{194}Os	332.7781	$3.98 \times 10^{+00}$
^{111}Ru	^{191}Os	330.5402	$9.85 \times 10^{+02}$	^{111}Ru	^{193}Os	330.4493	$4.19 \times 10^{+02}$
^{112}Ru	^{190}Os	331.6988	$6.78 \times 10^{+01}$	^{112}Ru	^{192}Os	331.7832	$1.92 \times 10^{+01}$
^{113}Rh	^{189}Re	334.1070	$1.04 \times 10^{+02}$	^{113}Rh	^{191}Re	333.3880	$1.63 \times 10^{+02}$
^{114}Pd	^{188}W	339.5190	1.89×10^{-01}	^{114}Pd	^{190}W	338.1410	$1.19 \times 10^{+00}$
^{115}Pd	^{187}W	337.6900	$7.29 \times 10^{+00}$	^{115}Pd	^{189}W	336.3160	$4.45 \times 10^{+01}$
^{116}Pd	^{186}W	339.7005	7.65×10^{-02}	^{116}Pd	^{188}W	338.7700	1.84×10^{-01}
^{117}Ag	^{185}Ta	340.9360	7.04×10^{-01}	^{117}Pd	^{187}W	336.5980	$1.55 \times 10^{+01}$
^{118}Cd	^{184}Hf	345.5620	2.87×10^{-03}	^{118}Pd	^{186}W	338.1672	4.21×10^{-01}
^{119}Cd	^{183}Hf	344.6200	1.79×10^{-02}	^{119}Ag	^{184}Ta	340.3100	5.54×10^{-01}
^{120}Cd	^{182}Hf	347.3670	3.00×10^{-05}	^{120}Cd	^{184}Hf	345.7270	3.62×10^{-04}
^{121}Cd	^{181}Hf	345.8366	7.75×10^{-04}	^{121}Cd	^{183}Hf	344.6238	3.42×10^{-03}
^{122}Cd	^{180}Hf	347.7517	7.40×10^{-06}	^{122}Cd	^{182}Hf	346.9324	1.34×10^{-05}
^{123}In	^{179}Lu	349.8490	5.36×10^{-06}	^{123}In	^{181}Lu	348.5000	3.31×10^{-05}
^{124}Sn	^{178}Yb	355.2892	6.67×10^{-10}	^{124}Sn	^{180}Yb	353.1042	3.82×10^{-08}
^{125}Sn	^{177}Yb	354.2428	7.56×10^{-09}	^{125}Sn	^{179}Yb	352.7064	7.97×10^{-08}
^{126}Sn	^{176}Yb	356.8663	4.86×10^{-12}	^{126}Sn	^{178}Yb	355.9800	9.90×10^{-12}
^{127}Sn	^{175}Yb	355.5266	1.55×10^{-10}	^{127}Sn	^{177}Yb	354.7274	2.51×10^{-10}
^{128}Sn	^{174}Yb	357.6665	3.32×10^{-13}	^{128}Sn	^{176}Yb	357.1233	2.87×10^{-13}
^{129}Sb	^{173}Tm	358.2450	6.85×10^{-12}	^{129}Sn	^{175}Yb	355.5566	1.36×10^{-11}
^{130}Te	^{172}Er	361.1969	1.36×10^{-13}	^{130}Sn	^{174}Yb	357.3467	1.50×10^{-13}
^{131}Sb	^{171}Tm	358.5517	1.72×10^{-12}	^{131}Sb	^{173}Tm	358.5074	3.27×10^{-13}
^{132}Te	^{170}Er	362.6567	1.02×10^{-14}	^{132}Sn	^{172}Yb	356.0719	1.33×10^{-12}
^{133}Te	^{169}Er	361.2202	7.06×10^{-14}	^{133}Te	^{171}Er	360.9261	3.86×10^{-14}
^{134}Xe	^{168}Dy	364.0458	3.31×10^{-14}	^{134}I	^{170}Ho	360.5530	2.45×10^{-12}
^{135}I	^{167}Ho	363.4201	1.08×10^{-14}	^{135}I	^{169}Ho	362.8461	1.13×10^{-14}
^{136}I	^{165}Ho	359.9763	4.92×10^{-11}	^{136}I	^{168}Ho	359.8750	1.10×10^{-11}
^{137}Xe	^{165}Dy	363.3560	1.12×10^{-13}	^{137}Xe	^{167}Dy	362.5834	1.45×10^{-13}
^{138}Xe	^{164}Dy	363.3002	1.12×10^{-13}	^{138}Xe	^{166}Dy	362.8270	6.50×10^{-14}
^{139}Cs	^{163}Tb	362.6570	9.07×10^{-12}	^{139}Cs	^{165}Tb	361.5410	3.03×10^{-11}
^{140}Ba	^{162}Gd	364.9090	1.73×10^{-13}	^{140}Ba	^{164}Gd	363.3090	2.12×10^{-12}
^{141}Ba	^{161}Gd	362.5988	7.17×10^{-11}	^{141}Ba	^{163}Gd	361.3170	3.55×10^{-10}
^{142}Ba	^{160}Gd	363.1437	1.59×10^{-11}	^{142}Ba	^{162}Gd	362.3920	1.97×10^{-11}
^{143}La	^{159}Gd	361.5750	3.71×10^{-09}	^{143}Ba	^{161}Gd	359.7128	1.59×10^{-08}

TABLE V. Table given below shows the probable cluster decay with half-lives comparable to α -decay half-lives.

Parent nuclei	Probable cluster	Daughter nuclei	Q value (MeV)	$T_{1/2}^{\text{cluster}}$ (s)	$T_{1/2}^{\alpha}$ (s)	Branching ratio
$^{290}\text{120}$	^{108}Pd	^{182}W	347.590	3.21×10^{-05}	1.23×10^{-05}	3.84×10^{-01}
	^{110}Pd	^{180}W	347.787	1.12×10^{-05}		$1.10 \times 10^{+00}$
	^{112}Pd	^{178}W	346.549	9.92×10^{-05}		1.24×10^{-01}
	^{113}Cd	^{177}Hf	351.744	2.20×10^{-05}		5.60×10^{-01}
$^{292}\text{120}$	^{110}Pd	^{182}W	346.457	6.00×10^{-05}	2.02×10^{-05}	3.37×10^{-01}
	^{115}Cd	^{177}Hf	350.845	2.64×10^{-05}		7.68×10^{-01}
$^{294}\text{120}$	^{87}Rb	^{207}Bi	318.933	6.10×10^{-05}	5.49×10^{-05}	9.00×10^{-01}
	^{114}Cd	^{180}Hf	350.344	2.87×10^{-05}		$1.91 \times 10^{+00}$
	^{117}Cd	^{177}Hf	349.849	4.03×10^{-05}		$1.36 \times 10^{+00}$
$^{296}\text{120}$	^{90}Sr	^{206}Pb	321.304	4.98×10^{-04}	5.42×10^{-04}	$1.09 \times 10^{+00}$
	^{117}Cd	^{179}Hf	348.451	2.49×10^{-04}		$2.18 \times 10^{+00}$
$^{298}\text{120}$	^{94}Sr	^{204}Pb	316.516	$1.56 \times 10^{+00}$	$1.28 \times 10^{+00}$	8.23×10^{-01}
	^{108}Ru	^{190}Os	334.929	$1.93 \times 10^{+00}$		6.63×10^{-01}
	^{113}Pd	^{185}W	339.539	$2.19 \times 10^{+00}$		5.86×10^{-01}
$^{300}\text{120}$	^{92}Sr	^{208}Pb	319.396	1.31×10^{-03}	1.01×10^{-03}	7.72×10^{-01}
	^{119}Cd	^{181}Hf	346.163	2.03×10^{-03}		4.99×10^{-01}
$^{302}\text{120}$	^{94}Sr	^{208}Pb	317.954	4.29×10^{-03}	1.52×10^{-03}	3.55×10^{-01}
	^{118}Cd	^{184}Hf	345.562	2.87×10^{-03}		5.30×10^{-01}
$^{304}\text{120}$	^{121}Cd	^{183}Hf	344.624	3.42×10^{-03}	6.65×10^{-03}	$1.95 \times 10^{+00}$

When we consider a SHN, there are chances for heavy-cluster decay if the predicted heavy-cluster half-life is comparable to the α -decay half-life. The main heavy clusters with half-life comparable with that of α , predicted from SHN $^{290\text{-}304}\text{120}$ in Table V are various isotopes cadmium ($Z = 48$) and palladium ($Z = 46$) both having proton number close to the magic number $Z = 50$. Another probable decay predicted is the rubidium leading to bismuth ($Z = 83$) daughter nucleus and various isotopes of strontium leading to lead ($Z = 82$) daughter nucleus. In our preliminary study on the decay of $^{290}\text{120}$ [49] and $^{304}\text{120}$ [50] the probable clusters emitted are found to be various isotopes of cadmium and palladium. In all these cases the predicted daughter nuclei have the proton numbers equal to or close to the magic number ($Z = 82$). It is worth trying to detect such decays with half-lives comparable to that of α decay. The role of the magic numbers in radioactive decay is evident here. Table VI represents the cluster-daughter combinations possible with the least half-lives among all splitting of each isotope of $^{290\text{-}304}\text{120}$. Decay chances are more probable when the half-life values are less. In most of the cases, the most probable cluster predicted in Table VI are found to be various isotopes of Ba, Ce, Xe, and Te with neutron number $N = 82$ or near to it. Other probable clusters predicted are ^{135}I ($N = 82$) and ^{137}Cs ($N = 82$) with magic numbers of neutrons. Thus, through our paper, we were able to detect a region where heavy particle emission is stronger than α decay and all the probable heavy clusters shown in Table VI have magic numbers of neutron ($N = 82$) or near to it. The present paper reveals that the decay chances are more probable to occur when either the emitted cluster or daughter nucleus is stable with magic numbers of protons or neutrons. In our previous work [38] on $^{288\text{-}296}\text{Og}$, the cluster emission with a half-life comparable α -decay half-life is indium ($Z = 49$) and cadmium ($Z = 48$), and the probable HPRs with least half-lives are ^{136}Xe and ^{138}Ba both having

$N = 82$. Thus, the role of the shell effect in nuclear decay is evident from our paper.

α decay occurs in heavy and superheavy nuclei, and we have experimental evidence for this [51,52]. Recently several theoretical investigations [53–55] are performed to study the chances of 2α emission from radioactive parent nuclei. Double α decay is the decay process where two α particles are emitted simultaneously from parent nuclei. The 2α decay can be assumed as a decay where two α particles tunnel through the potential barrier and gets emitted simultaneously. Or it can be imagined as the ^8Be nucleus to tunnel the potential barrier and to split to two α particles after crossing the barrier. In our paper we have calculated decay half-life for all possible cluster-daughter combinations from each isotope of $^{290\text{-}304}\text{120}$ and another interesting aspect we noted is that the half-life corresponding to the ^8Be decay is very less compared to the neighboring fragment combinations. In 1991, Poenaru *et al.* [56] observed that many of proton-rich SH nuclei including various isotopes of $Z = 120$ are ^8Be emitters. Since ^8Be is highly unstable, there is less chance for its emission. Hence, we have estimated the half-life of 2α decay using MGLDM with the Q -value-dependent preformation factor. Comparison of 2α and ^8Be emission from $^{290\text{-}304}\text{120}$ are shown in Table VII. Columns 1–4 in the table represent the parent nuclei, emitted cluster, daughter nuclei, and Q value, respectively. Column 5 represents the 2α decay half-life and ^8Be emission half-life from $^{290\text{-}304}\text{120}$ parent nuclei, and column 6 denotes the branching ratio of the 2α -decay half-life with respect to the α -decay half-life. From the table it is clear that the 2α half-lives are less than the ^8Be half-life, and the chances of 2α emissions are more. Also the 2α half-lives estimated are within the experimentally measurable range, and we request experimentalists to enhance experimental investigations in this region. We have also checked the chances of proton, two proton, neutron, and two neutron emissions from these parent

TABLE VI. Table shows the probable chances of heavy-cluster decay with minimum half-life among all possible splittings.

Parent nuclei	Probable cluster	Daughter nuclei	Q value (MeV)	$T_{1/2}^{\text{cluster}}$ (s)	Branching ratio
$^{290}\text{120}$	^{136}Ba ($N = 80$)	^{154}Gd ($N = 90$)	372.413	1.89×10^{-16}	$6.53 \times 10^{+10}$
	^{138}Ba ($N = 82$)	^{152}Gd ($N = 88$)	372.789	1.03×10^{-16}	$1.19 \times 10^{+11}$
$^{292}\text{120}$	^{136}Ba ($N = 80$)	^{156}Gd ($N = 92$)	371.302	3.84×10^{-16}	$5.27 \times 10^{+10}$
	^{138}Ba ($N = 82$)	^{154}Gd ($N = 90$)	371.848	1.60×10^{-16}	$1.27 \times 10^{+11}$
$^{294}\text{120}$	^{140}Ce ($N = 82$)	^{152}Sm ($N = 90$)	372.719	1.54×10^{-16}	$1.31 \times 10^{+11}$
	^{138}Ba ($N = 82$)	^{156}Gd ($N = 92$)	371.347	1.58×10^{-16}	$3.47 \times 10^{+11}$
$^{296}\text{120}$	^{140}Ce ($N = 82$)	^{154}Sm ($N = 92$)	371.081	7.97×10^{-16}	$6.89 \times 10^{+10}$
	^{132}Xe ($N = 78$)	^{164}Dy ($N = 98$)	366.817	8.31×10^{-15}	$6.53 \times 10^{+10}$
$^{298}\text{120}$	^{134}Xe ($N = 80$)	^{162}Dy ($N = 96$)	367.877	1.10×10^{-15}	$4.92 \times 10^{+11}$
	^{136}Xe ($N = 82$)	^{160}Dy ($N = 94$)	367.672	1.26×10^{-15}	$4.31 \times 10^{+11}$
$^{300}\text{120}$	^{137}Cs ($N = 82$)	^{159}Tb ($N = 94$)	367.648	6.12×10^{-15}	$8.87 \times 10^{+10}$
	^{138}Ba ($N = 82$)	^{160}Gd ($N = 96$)	368.763	8.92×10^{-16}	$1.44 \times 10^{+15}$
$^{302}\text{120}$	^{138}Ba ($N = 82$)	^{162}Gd ($N = 98$)	367.322	3.40×10^{-15}	$2.98 \times 10^{+11}$
	^{132}Te ($N = 80$)	^{170}Er ($N = 102$)	362.657	1.02×10^{-14}	$1.50 \times 10^{+11}$
$^{304}\text{120}$	^{133}Te ($N = 81$)	^{169}Er ($N = 101$)	361.220	7.06×10^{-14}	$2.16 \times 10^{+10}$
	^{134}Xe ($N = 80$)	^{168}Dy ($N = 102$)	364.046	3.31×10^{-14}	$4.60 \times 10^{+10}$
$^{304}\text{120}$	^{135}I ($N = 82$)	^{167}Ho ($N = 100$)	363.420	1.08×10^{-14}	$1.41 \times 10^{+11}$
	^{133}Te ($N = 81$)	^{171}Er ($N = 103$)	360.926	3.86×10^{-14}	$1.72 \times 10^{+11}$
$^{304}\text{120}$	^{135}I ($N = 82$)	^{169}Ho ($N = 102$)	362.846	1.13×10^{-14}	$5.88 \times 10^{+11}$
	^{138}Xe ($N = 84$)	^{166}Dy ($N = 100$)	362.827	6.50×10^{-14}	$1.02 \times 10^{+11}$

isotopes $^{290\text{--}304}\text{120}$ by calculating their proton and neutron separation energies [57] using the following expression:

$$S(p) = -\Delta M(A, Z) + \Delta M(A - 1, Z - 1) + \Delta M_H, \quad (14)$$

$$S(2p) = -\Delta M(A, Z) + \Delta M(A - 2, Z - 2) + 2\Delta M_H, \quad (15)$$

$$S(n) = -\Delta M(A, Z) + \Delta M(A - 1, Z) + \Delta M_n, \quad (16)$$

$$S(2n) = -\Delta M(A, Z) + \Delta M(A - 2, Z) + 2\Delta M_n. \quad (17)$$

Here $S(p)$, $S(2p)$, $S(n)$, and $S(2n)$ are the one-proton, two-proton, one-neutron, and two-neutron separation energies, respectively. $\Delta M(A, Z)$, ΔM_H , and ΔM_n are the mass excess

of the parent nucleus, one-proton, and one-neutron, respectively. $\Delta M(A-1, Z-1)$, $\Delta M(A-2, Z-2)$, $\Delta M(A-1, Z)$, and $\Delta M(A-2, Z)$ are the mass excess of daughter nucleus in one-proton, two-proton, one-neutron, and two-neutron radioactive decays, respectively. We calculated one-proton, two-proton ($2p$), one-neutron, and two-neutron separation energies using the above formula for parent isotopes $^{290\text{--}304}\text{120}$. Unfortunately all separation energies calculated are positive except for $2p$ emission from $^{290}\text{120}$. These findings show that all isotopes $^{290\text{--}304}\text{120}$ are stable against proton, neutron, and two-neutron decays. The only chance of decay is $2p$ emission from $^{290}\text{120}$. But the half-life predicted using MGLDM for the

TABLE VII. Possible chances of double alpha (2α) decay chances from parent nuclei $^{290\text{--}304}\text{120}$.

Parent nuclei	Emitted cluster	Daughter Nuclei	Q value (MeV)	$T_{1/2}^{\text{cluster}}$ (s)	Branching ratio
$^{290}\text{120}$	2α	^{282}Lv	25.1702	$1.47 \times 10^{+13}$	8.37×10^{-19}
	^8Be		25.0783	$2.15 \times 10^{+13}$	
$^{292}\text{120}$	2α	^{284}Lv	24.6202	$1.28 \times 10^{+14}$	1.58×10^{-19}
	^8Be		24.5283	$1.90 \times 10^{+14}$	
$^{294}\text{120}$	2α	^{286}Lv	24.1402	$8.94 \times 10^{+14}$	6.14×10^{-20}
	^8Be		24.0483	$1.35 \times 10^{+15}$	
$^{296}\text{120}$	2α	^{288}Lv	23.6902	$5.87 \times 10^{+15}$	9.24×10^{-20}
	^8Be		23.5983	$8.97 \times 10^{+15}$	
$^{298}\text{120}$	2α	^{290}Lv	22.5102	$1.46 \times 10^{+18}$	8.80×10^{-19}
	^8Be		22.4183	$2.32 \times 10^{+18}$	
$^{300}\text{120}$	2α	^{292}Lv	21.6902	$8.76 \times 10^{+19}$	1.16×10^{-23}
	^8Be		21.5983	$1.43 \times 10^{+20}$	
$^{302}\text{120}$	2α	^{294}Lv	22.9102	$1.50 \times 10^{+17}$	1.02×10^{-20}
	^8Be		22.8183	$2.35 \times 10^{+17}$	
$^{304}\text{120}$	2α	^{296}Lv	22.5502	$7.64 \times 10^{+17}$	8.70×10^{-21}
	^8Be		22.4583	$1.21 \times 10^{+18}$	

TABLE VIII. The comparison of α -decay half-life from $^{290-304}120$ using various theoretical models.

Parent nuclei	Q value (MeV)	$\log_{10}T_{1/2}^\alpha$ (s)						
		Present	Ref. [58]	Ref. [59]	UDL	UNIV	MB1	VSS
$^{290}120$	12.83508	-4.91		-4.61	-4.99	-5.17	-4.66	-4.90
$^{292}120$	12.71508	-4.69	-4.27	-4.17	-4.75	-4.96	-4.46	-4.65
$^{294}120$	12.49508	-4.26	-3.85	-3.71	-4.29	-4.55	-4.08	-4.18
$^{296}120$	12.22508	-3.70	-3.30	-3.85	-3.69	-4.03	-3.60	-3.58
$^{298}120$	10.67508	0.11	-1.97	-3.13	0.33	-0.39	-0.49	0.25
$^{300}120$	11.88508	-2.99	-2.60	-3.63	-2.93	-3.35	-2.81	-2.97
$^{302}120$	11.79508	-2.82	-2.43		-2.74	-3.18	-2.60	-2.80
$^{304}120$	11.51508	-2.18	-1.80		-2.06	-2.57	-1.93	-2.25

$2p$ decay from $^{290}120$ is 7.89×10^{152} s. Even though $2p$ decay from $^{290}120$ is found to be favored, the half-life predicted is so large, far above the experimental reach. Therefore, there is no chance to detect $2p$ decay from $^{290}120$.

We know that there exist many universal models or formulas to estimate half-lives of α decay. A comparison of the α decay half-life from $^{290-304}120$ using our present model with other theoretical models are shown in Table VIII. Columns 1–3 represents the parent nuclei, the Q value, and the logarithmic value of half-life in seconds using the present model MGLDM. The predicted half-life by Cui *et al.* [58] using effective liquid drop model inputting the Q value from KUY05 [45] is shown in column 4. α -decay half-lives predicted by Sayahi *et al.* [59] using the double folding potential is shown in column 5. The α -decay half-life predicted using the UDL [60], the universal curve (UNIV) [61], and the modified Brown formula (mB1) [62] is shown in columns 6–8. The Viola-Seaborg semiempirical formula (VSS), phenomenological formula of Viola and Seaborg [63] with constants determined by Sobiczewski *et al.* [64] is shown in the last column. From the table, it is evident that the half-lives predicted by our model are in agreement with other theoretical models and the predictions by the UDL give more matching results to our predictions. All the half-lives predicted using various models show similar trends with peak in the half-life at $^{298}120$. The isotope $^{298}120$ is an isotope of great interest with the magic number of protons ($Z = 120$) and semimagic number of neutrons ($N = 178$). The peak in half-life corresponds to the stability of parent nuclei and the role of magic number is evident from our paper.

A comparable α -decay half-life using various models does not mean that all these models give the same results when heavy cluster emission from the superheavy region is studied. For example, Zhang and Wang [36] studied the probable cluster radioactivity of $^{294}118$, $^{296}120$, and $^{298}122$ using the unified description formula, UNIV curve, Horoi formula, and UDL. The predictions by the first three models suggest that the probable emitted clusters are lighter nuclei, and the calculation within the UDL formula predicts both the lighter clusters and the heavier ones can be emitted from the parent nuclei. A further study on the competition between α decay and cluster radioactivity of $Z = 104-124$ isotopes is performed. The former three models predict that α decay is the dominant decay mode, but the UDL formula suggests that cluster decay dominates over α decay for $Z \geq 118$ nuclei and the isotopes

of $^{292-296,308-318}118$, $^{284-304,308-324}120$, and $^{316-322}122$ are the most likely candidates as the cluster emitters.

Decay chains of SHN $^{290-304}120$ are predicted by comparing $T_{1/2}^\alpha$ computed using the model MGLDM with $T_{1/2}^{\text{SF}}$ computed using the formula of Santhosh *et al.* [38], which depends on the mass inertia parameter (I_{rigid}) and is given below,

$$\log_{10}[T_{1/2}(\text{yr})] = c_1 + c_2 \left(\frac{Z^2}{(1 - kI^2)A} \right) + c_3 \left(\frac{Z^2}{(1 - kI^2)A} \right)^2 + c_4 E_{\text{shell}} + c_5 I_{\text{rigid}} + h_i, \quad (18)$$

where $I_{\text{rigid}} = B_{\text{rigid}}[1 + 0.31\beta_2 + 0.44\beta_2^2 + \dots]$ is the rigid body mass inertia of a nucleus [65,66] with the mass parameter $B_{\text{rigid}} = \frac{2}{5}MR^2 = 0.0138A^{5/3}(\hbar^2/\text{MeV})$ and $R = 1.2A^{1/3}$ (fm). Here M and β_2 are the mass of the nucleus and the quadrupole deformation, respectively. The constants in the new equation are obtained by fitting it to the experimental SF half-lives. The constants are $c_1 = 1208.763104$, $c_2 = -49.26439288$, $c_3 = 0.486222575$, $c_4 = 3.557962857$, and $c_5 = 0.04292571494$ with fixed value of $k = 2.6$ [67] and h_i is the blocking effect for the unpaired nucleon. For even-even heavy and superheavy nuclei $h_i = 0$, for odd- N nuclei $h_{eo} = 2.749814$, and for odd- Z nuclei $h_{oe} = 2.490760$. In our previous work, we have compared the experimental SF half-lives with the SF half-lives using mass inertia-dependent formulas for even-even, odd- N , and odd- Z superheavy nuclei (see Tables V and VI of Ref. [38]). The spontaneous fission half-life using the mass inertia-dependent SF equation agrees well with experimental observations. To validate the present calculations to calculate α half-life, we have calculated α -decay half-lives of the isotopes that appear in decay chains of $Z = 120$ isotopes whose experimental values are available and are shown in column 5 of Table IX. It is evident from table that model MGLDM is found to reproduce experimental half-lives of decay chains of $Z = 120$ and so without any doubt one can suggest that MGLDM can be used to study α -decay half-lives and decay chains of various isotopes of $Z = 120$.

Table IX predicts the modes of decay of even-even SHN in the range of $^{290-304}120$. Columns 1–4 denote the parent nuclei, the Q value, SF half-lives, and α -decay half-life, respectively. The SF half-life is calculated by the mass inertia-dependent expression of Santhosh *et al.* [38], and the α -decay half-life

TABLE IX. Table shows the modes of decay of isotopes $^{290-304}120$.

Parent nuclei	Q value (MeV)	Mode of decay			
		$T_{1/2}^{\text{SF}}(\text{s})$	$T_{1/2}^{\alpha}(\text{s})$	$T_{1/2}^{\text{Expt.}}(\text{s})$ [68]	Theory
$^{290}\text{L}20$	12.8351	$3.71 \times 10^{+02}$	1.23×10^{-05}		α
^{286}Og	12.3351	$3.81 \times 10^{+00}$	4.15×10^{-05}		α
^{282}Lv	12.4351	2.54×10^{-02}	7.41×10^{-06}		α
^{278}Fl	12.3051	2.26×10^{-03}	4.05×10^{-06}		α
^{274}Cn	13.1051	6.45×10^{-04}	3.21×10^{-08}		α
^{270}Ds	11.1151	1.87×10^{-03}	1.39×10^{-04}		α
^{266}Hs	10.3451	8.89×10^{-04}	2.87×10^{-03}		SF
$^{292}\text{L}20$	12.7151	$7.57 \times 10^{+03}$	2.02×10^{-05}		α
^{288}Og	11.9051	$3.06 \times 10^{+02}$	3.46×10^{-04}		α
^{284}Lv	11.8151	$3.24 \times 10^{+00}$	1.54×10^{-04}		α
^{280}Fl	13.3951	9.65×10^{-02}	2.74×10^{-08}		α
^{276}Cn	11.9051	7.09×10^{-04}	7.64×10^{-06}		α
^{272}Ds	10.7651	9.68×10^{-01}	9.08×10^{-04}		α
^{268}Hs	9.6251	2.79×10^{-01}	2.53×10^{-01}		SF/ α
^{264}Sg	9.2051	1.08×10^{-02}	9.89×10^{-01}		SF
$^{294}\text{L}20$	12.4951	$2.71 \times 10^{+05}$	5.49×10^{-05}		α
^{290}Og	11.6451	$8.36 \times 10^{+03}$	1.29×10^{-03}		α
^{286}Lv	11.1751	$1.89 \times 10^{+02}$	4.72×10^{-03}		α
^{282}Fl	12.6051	5.39×10^{-01}	8.38×10^{-07}		α
^{278}Cn	11.3051	3.76×10^{-06}	1.59×10^{-04}		SF
$^{296}\text{L}20$	12.2251	$2.06 \times 10^{+05}$	1.98×10^{-04}		α
^{292}Og	11.4651	$1.26 \times 10^{+05}$	3.21×10^{-03}		α
^{288}Lv	11.6851	$2.44 \times 10^{+03}$	2.62×10^{-04}		α
^{284}Fl	10.7951	$1.78 \times 10^{+00}$	1.02×10^{-02}		α
^{280}Cn	10.7351	1.51×10^{-06}	3.65×10^{-03}		SF
$^{298}\text{L}20$	10.6751	$2.58 \times 10^{+05}$	$1.28 \times 10^{+00}$		α
^{294}Og	11.8351	$1.44 \times 10^{+05}$	3.96×10^{-04}	6.90×10^{-04}	α
^{290}Lv	11.0051	$2.17 \times 10^{+04}$	1.08×10^{-02}	8.30×10^{-03}	α
^{286}Fl	10.3651	$4.83 \times 10^{+01}$	1.31×10^{-01}	1.20×10^{-01}	α
^{282}Cn	10.1751	1.66×10^{-04}	1.04×10^{-01}	9.10×10^{-04}	SF
$^{300}\text{L}20$	11.8851	$2.02 \times 10^{+04}$	1.01×10^{-03}		α
^{296}Og	9.8051	$1.62 \times 10^{+06}$	$9.73 \times 10^{+01}$		α
^{292}Lv	10.7751	$9.33 \times 10^{+05}$	3.91×10^{-02}	1.30×10^{-02}	α
^{288}Fl	10.0651	$3.03 \times 10^{+03}$	8.39×10^{-01}	6.60×10^{-01}	α
^{284}Cn	9.6051	1.35×10^{-02}	$4.31 \times 10^{+00}$	9.80×10^{-02}	SF
$^{302}\text{L}20$	11.7951	$7.58 \times 10^{+02}$	2.68×10^{-09}		α
^{298}Og	11.1151	$1.55 \times 10^{+05}$	1.88×10^{-02}		α
^{294}Lv	10.1651	$4.34 \times 10^{+06}$	$1.72 \times 10^{+00}$		α
^{290}Fl	9.0551	$2.14 \times 10^{+05}$	$1.09 \times 10^{+03}$		α
^{286}Cn	8.7351	5.23×10^{-01}	$2.77 \times 10^{+03}$		SF
$^{304}\text{L}20$	11.5151	$3.55 \times 10^{+00}$	6.65×10^{-03}		α
^{300}Og	11.0351	$7.56 \times 10^{+03}$	2.79×10^{-02}		α
^{296}Lv	10.5051	$2.13 \times 10^{+06}$	1.77×10^{-01}		α
^{292}Fl	8.3751	$7.99 \times 10^{+06}$	$2.83 \times 10^{+05}$		α
^{288}Cn	8.4751	$2.20 \times 10^{+00}$	$2.21 \times 10^{+04}$		SF

is calculated using our model MGLDM. Column 5 denotes the experimental half-lives taken from Ref. [68]. Columns 6 and 7 denote the theoretical and experimental modes of decay. The daughter nucleus of ^{290}Zr , such as ^{286}Og , ^{282}Lv , ^{278}Fl , ^{274}Cn , and ^{270}Ds have α half-lives lower than spontaneous fission half-life and, hence, can survive the fission process. For the daughter nucleus ^{266}Hs , the spontaneous fission half-life is lower than the α half-life and, thus, spontaneous fission occurs. Thus our paper predicts ^{290}Zr decays by six α chains followed by spontaneous fission. For the parent nucleus ^{292}Zr for the first six cases, the α half-life is less than SF half-lives. Then, for the daughter nucleus ^{268}Hs both the α half-life and the SF half-life are comparable. Then, for ^{264}Sg , the α half-life is greater than the SF half-life, and spontaneous fission occurs. Thus, ^{292}Zr decays by six α chains followed by spontaneous fission. For the other isotopes of SHN, $^{294,296,298,300,302,304}\text{Zr}$ decays by four α chains followed by spontaneous fission. The experimental half-life available and the mode of decay that can be predicted using experimentally available values also supports our predictions. From the predicted half-life it is noteworthy that some daughter nucleus has α half-life greater than its neighbor nucleus in the decay chain. In such cases either the daughter nucleus will be more stable or have chances for spontaneous fission to occur. For the parent nucleus ^{300}Zr , daughter nucleus ^{296}Og is found to have a greater half-life than its neighbors but less than the spontaneous fission half-life. Hence, ^{296}Og is expected to

more stable, and experimentalists could conduct experiments to synthesize this nucleus in the near future. For the parent nuclei $^{296,298,304}\text{Zr}$, daughter nuclei ^{284}Fl , ^{286}Fl , and ^{292}Fl are found to have greater half-lives than its neighbors and can be considered as more stable.

IV. CONCLUSION

In our present paper, we have investigated all probable chances of decay from even-even SHN with atomic number $Z = 120$ and mass number varying from 290 to 304, such as α decay, double α decay, cluster decay, spontaneous fission, proton decay, neutron decay, etc. In our paper, we have also calculated the chances of cluster emission from each isotope of $^{290-304}\text{Zr}$ with half-lives comparable to the α -decay half-life and the probable cluster decay with minimum half-life. Interestingly for the predicted cluster decay, either the cluster predicted or the daughter nuclei are found to be stable with magic numbers of protons or neutrons or near to it. Nuclear decay is more probable to occur when any of the decay products or both are stable. We have also predicted the modes of decay of $^{290-304}\text{Zr}$ isotopes by comparing the α -decay half-life with the SF half-life. We hope that our paper has great importance as scientists are taking greater efforts to experiments near the limits of nuclear stability, such as production of new stable heavy isotopes.

-
- [1] S. Hofmann and G. Münzenberg, *Rev. Mod. Phys.* **72**, 733 (2000).
 - [2] S. Hofmann, V. Ninov, F. P. Heßberger, P. Armbruster, H. Folger, G. Münzenberg, H. J. Schött, A. G. Popeko, A. V. Yeremin, A. N. Andreyev, and S. Saro, *Z. Phys. A: Hadrons Nucl.* **350**, 277 (1995).
 - [3] S. Hofmann, V. Ninov, F. P. Heßberger, P. Armbruster, H. Folger, G. Münzenberg, H. J. Schött, A. G. Popeko, A. V. Yeremin, A. N. Andreyev, and S. Saro, *Z. Phys. A: Hadrons Nucl.* **350**, 281 (1995).
 - [4] S. Hofmann, V. Ninov, F. P. Heßberger, P. Armbruster, H. Folger, G. Münzenberg, H. J. Schött, A. G. Popeko, A. V. Yeremin, S. Saro, and R. Janik, *Z. Phys. A: Hadrons Nucl.* **354**, 229 (1996).
 - [5] S. Hofmann, *Rep. Prog. Phys.* **61**, 639 (1998).
 - [6] S. Hofmann, *Acta Phys. Pol. B* **30**, 621 (1999).
 - [7] K. Morita, K. Morimoto, D. Kaji, T. Akiyama, S. I. Goto, H. Haba, E. Ideguchi, R. Kanungo, K. Katori, H. Koura, and H. Kudo, *J. Phys. Soc. Jpn.* **73**, 2593 (2004).
 - [8] Y. T. Oganessian, V. K. Utyonkov, Y. V. Lobanov, F. S. Abdullin, A. N. Polyakov, I. V. Shirokovsky, Y. S. Tsyanov, G. G. Gulbekian, S. L. Bogomolov, B. N. Gikal, A. N. Mezentsev, S. Iliev, V. G. Subbotin, A. M. Sukhov, G. V. Buklanov, K. Subotic, M. G. Itkis, K. J. Moody, J. F. Wild, N. J. Stoyer, M. A. Stoyer, and R. W. Lougheed, *Phys. Rev. Lett.* **83**, 3154 (1999).
 - [9] Yu. Ts. Oganessian, *Nucl. Phys. A* **685**, 17 (2001).
 - [10] Y. T. Oganessian, V. K. Utyonkov, Y. V. Lobanov, F. S. Abdullin, A. N. Polyakov, I. V. Shirokovsky, Y. T. Tsyanov, G. G. Gulbekian, S. L. Bogomolov, A. N. Mezentsev, and S. Iliev, *Phys. Rev. C* **69**, 021601(R) (2004).
 - [11] Y. T. Oganessian, *J. Phys. G: Nucl. Part. Phys.* **34**, R165 (2007).
 - [12] Y. T. Oganessian, F. S. Abdullin, P. D. Bailey, D. E. Benker, M. E. Bennett, S. N. Dmitriev, J. G. Ezold, J. H. Hamilton, R. A. Henderson, M. G. Itkis, and Y. V. Lobanov, A. N. Mezentsev, K. J. Moody, S. L. Nelson, A. N. Polyakov, C. E. Porter, A. V. Ramayya, F. D. Riley, J. B. Roberto, M. A. Ryabinin, K. P. Rykaczewski, R. N. Sagaidak, D. A. Shaughnessy, I. V. Shirokovsky, M. A. Stoyer, V. G. Subbotin, R. Sudowe, A. M. Sukhov, Y. S. Tsyanov, V. K. Utyonkov, A. A. Voinov, G. K. Vostokin, and P. A. Wilk, *Phys. Rev. Lett.* **104**, 142502 (2010).
 - [13] R. Eichler, N. V. Aksenov, A. V. Belozerov, G. A. Bozhikov, V. I. Chepigin, R. Dressler, S. N. Dmitriev, H. W. Gäggeler, V. A. Gorshkov, F. Haenssler, and M. G. Itkis, *Nucl. Phys. A* **787**, 373 (2007).
 - [14] Y. T. Oganessian, F. S. Abdullin, P. D. Bailey, D. E. Benker, M. E. Bennett, S. N. Dmitriev, J. G. Ezold, J. H. Hamilton, R. A. Henderson, M. G. Itkis, Y. V. Lobanov, A. N. Mezentsev, K. J. Moody, S. L. Nelson, A. N. Polyakov, C. E. Porter, A. V. Ramayya, F. D. Riley, J. B. Roberto, M. A. Ryabinin, K. P. Rykaczewski, R. N. Sagaidak, D. A. Shaughnessy, I. V. Shirokovsky, M. A. Stoyer, V. G. Subbotin, R. Sudowe, A. M. Sukhov, R. Taylor, Y. S. Tsyanov, V. K. Utyonkov, A. A. Voinov, G. K. Vostokin, and P. A. Wilk, *Phys. Rev. C* **83**, 054315 (2011).
 - [15] V. I. Zagrebaev and W. Greiner, *Nucl. Phys. A* **944**, 257 (2015).
 - [16] Y. T. Oganessian, V. K. Utyonkov, Y. V. Lobanov, F. S. Abdullin, A. N. Polyakov, R. N. Sagaidak, I. V. Shirokovsky, Y. S. Tsyanov, A. A. Voinov, A. N. Mezentsev, V. G. Subbotin, A. M. Sukhov, K. Subotic, V. I. Zagrebaev, S. N. Dmitriev, R. A. Henderson, K. J. Moody, J. M. Kenneally, J. H. Landrum,

- D. A. Shaughnessy, M. A. Stoyer, N. J. Stoyer, and P. A. Wilk, *Phys. Rev. C* **79**, 024603 (2009).
- [17] S. Hofmann, S. Heinz, R. Mann, J. Maurer, G. Munzenberg, S. Antalic, W. Barth, H. G. Burkhardt, L. Dahl, K. Eberhardt, R. Grzywacz, J. H. Hamilton, R. A. Henderson, J. M. Kenneally, B. Kindler, I. Kojouharov, R. Lang, B. Lommel, K. Miernik, D. Miller, K. J. Moody, K. Morita, K. Nishio, A. G. Popeko, J. B. Roberto, J. Runke, K. P. Rykaczewski, S. Saro, C. Scheidenberger, H. J. Schott, D. A. Shaughnessy, M. A. Stoyer, P. Thorle-Pospiech, K. Tinschert, N. Trautmann, J. Uusitalo, and A. V. Yeremin, *Eur. Phys. J. A* **52**, 180 (2016).
- [18] R. A. Gherghescu and N. Carjan, *J. Phys. G: Nucl. Part. Phys.* **36**, 025106 (2009).
- [19] S. Ahmed, M. Bhuyan, and S. K. Patra, *Int. J. Mod. Phys. E* **21**, 1250092 (2012).
- [20] K. P. Santhosh and B. Priyanka, *Nucl. Phys. A* **929**, 20 (2014).
- [21] G. Saxena, A. Jain, and P. K. Sharma, *Phys. Scr.* **96**, 125304 (2021).
- [22] P. B. Price, *Annu. Rev. Nucl. Part. Sci.* **39**, 19 (1989).
- [23] E. Hourani, M. Hussonnoisand, and D. N. Poenaru, *Ann. Phys. (Paris)* **14**, 311 (1989).
- [24] S. S. Malik, S. Singh, R. K. Puri, S. Kumar, and R. K. Gupta, *Pramana* **32**, 419 (1989).
- [25] D. N. Poenaru, W. Greiner, M. Ivascu, and A. Sandulescu, *Phys. Rev. C* **32**, 2198 (1985).
- [26] D. N. Poenaru, R. A. Gherghescu, and W. Greiner, *Phys. Rev. Lett.* **107**, 062503 (2011).
- [27] D. N. Poenaru, R. A. Gherghescu, and W. Greiner, *Phys. Rev. C* **83**, 014601 (2011).
- [28] D. N. Poenaru, R. A. Gherghescu, and W. Greiner, *Phys. Rev. C* **85**, 034615 (2012).
- [29] A. V. Karpov, V. I. Zagrebaev, W. Greiner, L. F. Ruiz, and Y. M. Palenzuela, *Int. J. Mod. Phys. E* **21**, 1250013 (2012).
- [30] C. Qi, F. R. Xu, R. J. Liotta, R. Wyss, M. Y. Zhang, C. Asawatangtrakuldee, and D. Hu, *Phys. Rev. C* **80**, 044326 (2009).
- [31] D. Ni, Z. Z. Ren, T. K. Dong, and C. Xu, *Phys. Rev. C* **78**, 044310 (2008).
- [32] M. Horoi, *J. Phys. G: Nucl. Part. Phys.* **30**, 945 (2004).
- [33] C. Nithya and K. P. Santhosh, *Nucl. Phys.* **1020**, 122400 (2022).
- [34] D. N. Poenaru, H. Stöcker, and R. A. Gherghescu, *Eur. Phys. J. A* **54**, 14 (2018).
- [35] D. N. Poenaru and R. A. Gherghescu, *Europhys. Lett.* **124**, 52001 (2018).
- [36] Y. L. Zhang and Y. Z. Wang, *Phys. Rev. C* **97**, 014318 (2018).
- [37] K. P. Santhosh and C. Nithya, *Phys. Rev. C* **97**, 064616 (2018).
- [38] K. P. Santhosh, Tinu Ann Jose, and N. K. Deepak, *Phys. Rev. C* **103**, 064612 (2021).
- [39] J. Blocki, J. Randrup, W. J. Swiatecki, and C. F. Tsang, *Ann. Phys. (NY)* **105**, 427 (1977).
- [40] J. Blocki and W. J. Swiatecki, *Ann. Phys. (NY)* **132**, 53 (1981).
- [41] K. P. Santhosh and Tinu Ann Jose, *Phys. Rev. C* **99**, 064604 (2019).
- [42] G. Royer and B. Remaud, *J. Phys. G: Nucl. Part. Phys.* **10**, 1057 (1984).
- [43] G. Royer and B. Remaud, *Nucl. Phys. A* **444**, 477 (1985).
- [44] M. Wang, G. Audi, F. G. Kondev, W. J. Huang, S. Naimi, and X. Xu, *Chin. Phys. C* **41**, 030003 (2017).
- [45] H. Koura, T. Tachibana, M. Uno, and M. Yamada, *Prog. Theor. Phys.* **113**, 305 (2005).
- [46] K. P. Santhosh and I. Sukumaran, *Can. J. Phys.* **95**, 31 (2017).
- [47] N. Wang, M. Liu, X. Wu, and J. Meng, *Phys. Rev. C* **93**, 014302 (2016).
- [48] T. A. Siddiqui, A. Quddus, S. Ahmad, and S. K. Patra, *J. Phys. G: Nucl. Part. Phys.* **47**, 115103 (2020).
- [49] Tinu Ann Jose, K. P. Santhosh, and N. K. Deepak, in *Proceedings of 34th Kerala Science Congress, Thiruvananthapuram, India, 2022* (Kerala Science Congress, Thiruvananthapuram, India), p. 432.
- [50] Tinu Ann Jose and K. P. Santhosh, in *Proceedings of 65th DAE-BRNS Symposium on Nuclear Physics, Mumbai, India, 2021* (BARC, Mumbai, India), Vol. 65, p. 275.
- [51] Y. T. Oganessian, V. K. Utyonkov, Y. V. Lobanov, F. S. Abdullin, A. N. Polyakov, I. V. Shirokovsky, Y. S. Tsyganov, G. G. Gulbekian, S. L. Bogomolov, B. N. Gikal, A. N. Mezentsev, S. Iliev, V. G. Subbotin, A. M. Sukhov, A. A. Voinov, G. V. Buklanov, K. Subotic, V. I. Zagrebaev, M. G. Itkis, J. B. Patin, K. J. Moody, J. F. Wild, M. A. Stoyer, N. J. Stoyer, D. A. Shaughnessy, J. M. Kenneally, P. A. Wilk, R. W. Lougheed, R. I. Il'kaev, and S. P. Vesnovskii, *Phys. Rev. C* **70**, 064609 (2004).
- [52] Y. T. Oganessian, V. K. Utyonkov, Y. V. Lobanov, F. S. Abdullin, A. N. Polyakov, I. V. Shirokovsky, Y. T. Tsyganov, G. G. Gulbekian, S. L. Bogomolov, B. N. Gikal, A. N. Mezentsev, S. Iliev, V. G. Subbotin, A. M. Sukhov, A. A. Voinov, G. V. Buklanov, K. Subotic, V. I. Zagrebaev, M. G. Itkis, J. B. Patin, K. J. Moody, J. F. Wild, M. A. Stoyer, N. J. Stoyer, D. A. Shaughnessy, J. M. Kenneally, P. A. Wilk, R. W. Lougheed, R. I. Il'kaev, and S. P. Vesnovskii, *Phys. Rev. C* **71**, 029902(E) (2005).
- [53] D. N. Poenaru and M. Ivascu, *J. Phys. Lett.* **46**, 591 (1985).
- [54] V. I. Tretyak, *Nucl. Phys. At. Energy* **22**, 121 (2021).
- [55] K. P. Santhosh and T. A. Jose, *Phys. Rev. C* **104**, 064604 (2021).
- [56] D. N. Poenaru, D. Schnabel, W. Greiner, D. Mazilu, and R. Gherghescu, *At. Data Nucl. Data Tables* **48**, 231 (1991).
- [57] S. Athanassopoulos, E. Mavrommatis, K. A. Gernoth, and J. W. Clark, [arXiv:nucl-th/0509075](https://arxiv.org/abs/nucl-th/0509075).
- [58] J. P. Cui, Y. L. Zhang, S. Zhang, and Y. Z. Wang, *Phys. Rev. C* **97**, 014316 (2018).
- [59] M. Sayahi, V. Dehghani, D. Naderi, and S. A. Alavi, *Z. Naturforsch. A: Phys. Sci.* **74**, 551 (2019).
- [60] C. Qi, F. R. Xu, R. J. Liotta, and R. Wyss, *Phys. Rev. Lett.* **103**, 072501 (2009).
- [61] D. N. Poenaru and W. Greiner, *Phys. Scr.* **44**, 427 (1991).
- [62] A. I. Budaca, R. Budaca, and I. Silisteanu, *Nucl. Phys. A* **951**, 60 (2016).
- [63] V. E. Viola, Jr. and G. T. Seaborg, *J. Inorg. Nucl. Chem.* **28**, 741 (1966).
- [64] A. Sobiczewski, Z. Patyk, and S. Cwiok, *Phys. Lett. B* **224**, 1 (1989).
- [65] A. Bohr and B. R. Mottelson, *Mat. Fys. Medd.-K. Dan. Vidensk. Selsk.* **30**, 1 (1955).
- [66] J. M. Allmond and J. L. Wood, *Phys. Lett. B* **767**, 226 (2017).
- [67] X. J. Bao, S. Q. Guo, H. F. Zhang, Y. Z. Xing, J. M. Dong, and J. Q. Li, *J. Phys. G: Nucl. Part. Phys.* **42**, 085101 (2015).
- [68] Y. T. Oganessian, A. Sobiczewski, and G. M. Ter-Akopian, *Phys. Scr.* **92**, 023003 (2017).